

Targeted nanopore sequencing by real-time mapping of raw electrical signal with UNCALLED

Sam Kovaka¹, Yunfan Fan², Bohan Ni¹, Winston Timp², Michael C. Schatz^{1,3,4}

1. Department of Computer Science, Johns Hopkins University, Baltimore, MD
2. Department of Biomedical Engineering, Johns Hopkins University, Baltimore, MD
3. Department of Biology, Johns Hopkins University, Baltimore, MD
4. Cold Spring Harbor Laboratory, Cold Spring Harbor, NY

Abstract

ReadUntil sequencing allows nanopore devices to selectively eject individual reads from the pore in real-time. This could enable purely computational targeted sequencing, however most mapping methods require basecalling, which is computationally intensive. Here we present UNCALLED (github.com/skovaka/UNCALLED), an open-source mapper that rapidly matches streaming nanopore current signals to a reference sequence. UNCALLED probabilistically considers k-mers that the signal could represent, and then prunes the candidates based on the reference encoded within an FM-index. We used UNCALLED to deplete sequencing of known bacterial genomes within a metagenomics community, enriching the remaining species by 4.46 fold. UNCALLED also enriched 148 human genes associated with hereditary cancers to 29.6x coverage using one MinION flowcell, enabling accurate detection of SNPs, indels, structural variants (SVs), and methylation in these genes. Twice as many SVs were detected compared to 50x coverage Illumina sequencing, verified by whole-genome nanopore and PacBio HiFi sequencing.

Introduction

High-throughput long-read sequencers from Oxford Nanopore Technologies (ONT) produce millions of reads that are several thousand nucleotides in length in a single 48 to 72 hour run. These reads are able to span regions that are otherwise difficult to resolve using conventional short-read sequencing, offering the ability to produce highly contiguous genome assemblies, even spanning centromeric repeats¹, identify structural variants with significantly higher accuracy, and sequence tens to hundreds of thousands of full-length RNA transcripts in a single run². Nanopore reads can also be used to identify nucleotide modifications, such as methylation, without any additional library preparation considerations³.

Nanopore sequencing operates by measuring ionic current as a nucleotide strand passes through a pore. The specific nucleotides in the pore modulate the current in characteristic ways, which can be used to infer individual nucleotides via basecalling of the raw current signal data. For the R9.4 pore, the current is primarily affected by six nucleotides in the central constriction of the pore, which produce signals ranging from 60 to 120 picoamps (pA). Single molecule current readings at these levels are noisy, making it difficult to determine the identity of an individual k-mer. However, by combining the signal information across multiple overlapping k-mers, state-of-the-art basecallers, such as Guppy, can achieve read identities averaging approximately 90%⁴. However, this process is computationally intensive and requires several days to basecall on a high-end multicore CPU. A high-yield run can take well over 24 hours to complete even with a GPU (graphics processing unit).

The ONT MinION is a hand-held low-cost sequencer which typically produces 10-20 Gbp of data from a single standard flowcell. The low price and portability of the MinION has enabled rapid sequencing in remote areas without the need to ship DNA to a sequencing facility⁵. Reads from the sequencer can be output, basecalled, and analyzed as soon as a run begins, which along with the relatively simple library preparation could make rapid sequencing-based diagnostics widely available⁶. The recently released Flongle (flowcell dongle) further improves the accessibility of nanopore sequencing by enabling the use of less expensive flowcells, although this reduces the MinION's throughput to ~2Gbp. Though this throughput has enjoyed a steady improvement since the initial release of the instrument in 2014, many applications require higher depth, making targeted sequencing necessary. Notably, 20Gbps of data is only approximately 6.6x coverage of a human genome, which is insufficient for most forms of variant calling thereby increasing costs for whole human genome analysis^{7,8}.

Typical targeted sequencing methods such as PCR are not suitable for many nanopore sequencing applications. PCR has difficulty amplifying DNA fragments larger than 5Kbp to 30Kbp, which limits nanopore runs that could otherwise produce reads well over 100Kbp. Furthermore, amplification erases nucleotide modifications, which nanopore sequencing could otherwise identify^{3,9}. Enrichment methods specifically designed for nanopore sequencing like hybrid capture or CRISPR/Cas9 enrichment alleviate some of these issues, however, they require specialized reagents and extra preparation time¹⁰. These approaches are also limited in the maximum number and size of regions that can be simultaneously targeted without excessive numbers of reactions and can yield inconsistent amounts of coverage when tiling large regions.

As an alternative, ONT devices have a unique method for real-time targeted sequencing known as ReadUntil, where an individual pore can selectively eject a read while sequencing¹¹. This is accomplished by reversing the polarity of the voltage across the specified pore for a short period of time

(~0.1s) to eject the molecule and allow a new sequencing read to begin sooner. If one can identify reads that are not of interest and eject them quickly enough, this can enrich the sequencing for targeted regions via a purely computational technique. ReadUntil is more effective with longer reads because each ejection avoids sequencing more nucleotides than if the reads were shorter. For example, the longest reported Nanopore read exceeded 2Mbp in length, and required over 1 hour of sequencing¹². If this read originated from an off-target region, the sequencing capacity of that pore is effectively wasted for the entire hour, while ReadUntil could have reclaimed that capacity within a few seconds.

In addition to enriching known targets, ReadUntil can instead be used to deplete sequencing of uninteresting or unwanted regions. For example, this could be used to exclude the sequencing of a known microbe in a metagenomics sample or exclude high copy organelles from a plant or animal sample. This is analogous to CRISPR/Cas9-based methods which deplete unwanted sequences¹³, where again ReadUntil has the benefit of not requiring additional library preparation and can uniformly deplete entire genomes as needed. The dynamic nature of ReadUntil could also be utilized to deplete certain sequences after they have been sequenced to a desired depth, which could be useful in metagenomic applications and genome assembly.

A MinION device can sequence up to 512 molecules at a rate of 450 nucleotides per second, requiring a very fast algorithm to effectively enrich regions of interest with ReadUntil. Previous work to enable ReadUntil sequencing used a signal level analysis technique called dynamic time warping to align raw nanopore signal to an *in silico* signal representation of a reference sequence, but this method does not scale to references larger than tens of kilobases as the runtime is quadratic in the length of the sequence¹¹. Others have attempted basecalling followed by mapping with a DNA aligner^{14,15}, but basecalling is computationally expensive, and most basecallers are designed to work with fully sequenced reads and require a sizable amount of input signal to output a sequence. A ReadUntil method should ideally be fully streaming, meaning it can continuously refine its classification as more signal is produced. **It would also be desirable to have a method that can continue to scale in the future as yields increase with highly parallel devices like the PromethION.**

To address these issues, we have developed UNCALLED, the Utility for Nanopore Current ALignment to Large Expanses of DNA, with the goal of mapping streaming raw signal to DNA references for targeted sequencing using ReadUntil. UNCALLED uses the FM-index¹⁶ to search for sequences in a DNA reference that are consistent with possible k-mers that the raw signal could represent (**Fig. 1a**). It first converts the raw signal into events, which are stretches of signal that approximate k-mer boundaries, and then calculates the probability that each event matches each possible k-mer using a probabilistic model released by ONT. High-probability k-mers are used as a query in a novel FM-index

search algorithm developed for UNCALLED which considers all possible sequences and locations for each event as the mapping progresses (**Supplemental Fig. S1**). The probability cutoff used to decide if a k-mer should be considered is dynamically adjusted depending on how many locations a potential sequence could map to, which maintains both high accuracy and high speed when mapping the noisy signal data (**Supplemental Fig. S2**). Finally, a seed clustering algorithm filters out false positive locations by grouping seeds together that map to consistent positions, and a final mapping is reported once a single location has sufficiently more support than the alternatives. We show that UNCALLED can map reads to collections of whole bacterial genomes as fast as a full MinION flowcell can produce reads, and can enrich target genomes by several fold compared to a control. We also show UNCALLED can enrich sequencing a panel of 148 human genes associated with hereditary cancer to a mean of 29.6x on-target coverage, compared to 5.3x coverage on a matched control flowcell, which enables highly precise and sensitive detection of single nucleotide variants, small insertions and deletions, structural variants (SVs), and DNA methylation. Notably, SV calls from enriched UNCALLED reads have 100% concordance with whole-genome ONT and PacBio HiFi sequencing, and detect more than twice the number of SVs compared to whole-genome Illumina sequencing.

Results

Mapping *Escherichia coli* reads

To measure the accuracy and efficiency of UNCALLED we mapped the raw signal of 100,000 *Escherichia coli* reads to the *E. coli* K12 reference genome using a single 3.0 GHz core. The reads were previously sequenced using a MinION³ and have an average length of ~5Kbp. Only the first 30,000 events (~15Kbp worth of signal) at most were considered for each read, which is a default cutoff when using UNCALLED to map previously sequenced reads to avoid spending too much time on exceptionally long reads. Of the reads that mapped, UNCALLED processed a median of 10 kilobases worth of signal per second, the equivalent of 22 actively sequencing pores per thread, and most reads were mapped in under 50 milliseconds (**Fig. 1b**). Of the reads that UNCALLED successfully mapped, 75% were mapped within one second's worth of sequencing (450bp), which is the amount of signal that the ReadUntil API provides per chunk (**Fig. 1c**). To estimate accuracy we used minimap2¹⁷ alignments of the basecalled reads as a ground truth: reads that map to the same location are classified as True Positives (TP), reads that neither tool map are True Negatives (TN), reads that are either not mapped by minimap2 or were mapped to a different location than UNCALLED are False Positives (FP), and reads that UNCALLED did not map but minimap2 did are False Negatives (FN). The overall accuracy (TP+TN) of UNCALLED by this analysis was 93.7%. We found that the quality scores (Q scores) of the false negative and false positive reads are much lower than the true positives (**Supplemental Table S1**). Furthermore, 75% of “false positives” consisted of reads that were not aligned by minimap2,

meaning the UNCALLED location could be correct and minimap2 could not find it. In addition, of the false positives that minimap2 did align, 92% are explained by repeats: according to nucmer¹⁸ self-genome alignments, the reference location that UNCALLED mapped to was a high-identity repeat of the minimap2 reference location. Without repeat masking this type of error is unavoidable if ReadUntil mapping is the goal, since we attempt to find a position based on as little of the read as possible, while minimap2 can consider the full sequence of the read.

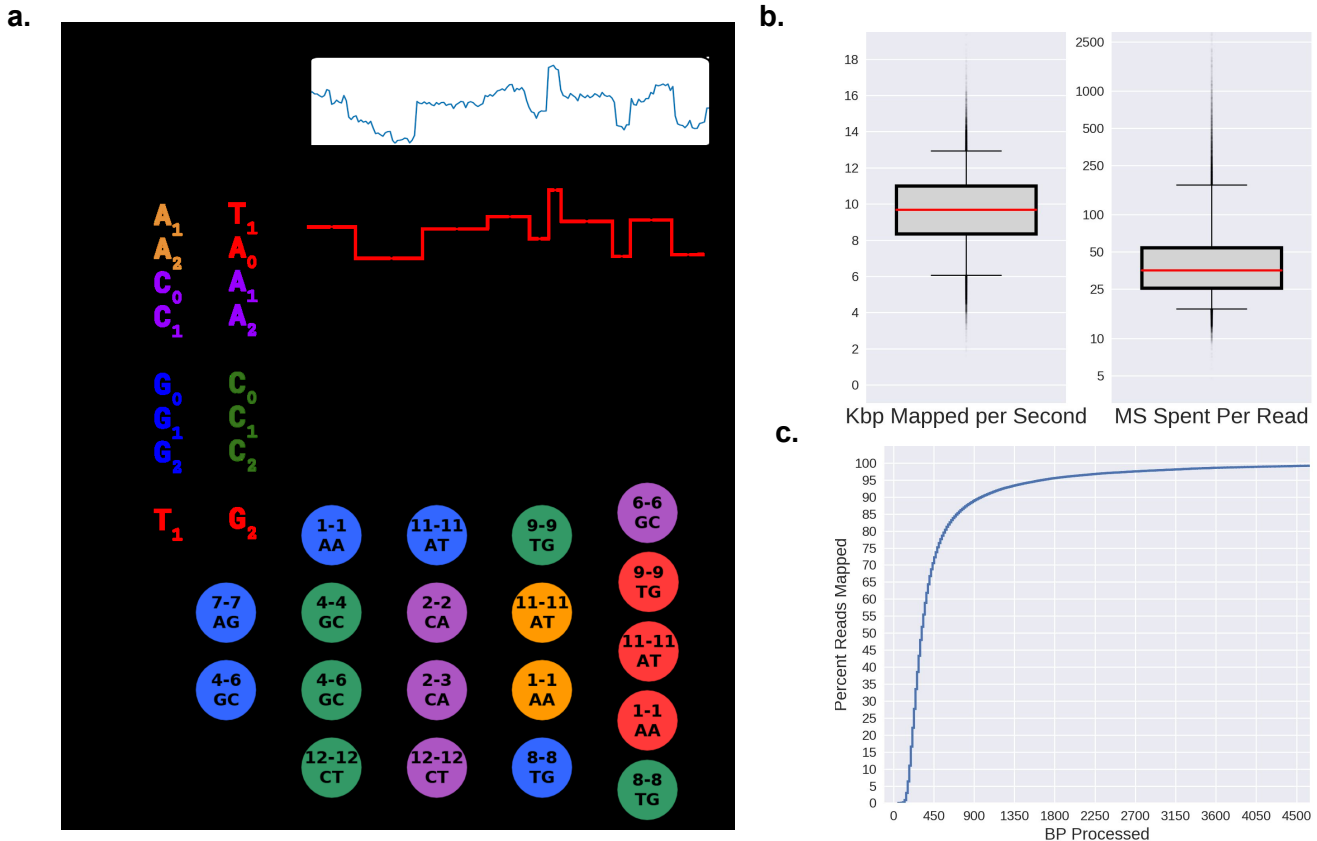


Figure 1. UNCALLED algorithm and performance on *Escherichia coli* data. **(a)** Overview of the algorithm: inputs are an FM index built from the DNA reference, and the raw nanopore signal. The signal is converted to events, and the log probabilities of events matching each k-mer is computed. All paths through the FM-index that are consistent with k-mers that match each event above a threshold are searched, conceptually forming a forest of trees (Supplemental Fig. S1 for more details). **(b)** Boxplots showing the speed of UNCALLED mapping *E. coli* reads to the *E. coli* K12 reference genome in kilobases per second (left) and total number of milliseconds required to map reads (right). Center lines represent the median, box limits represent upper and lower quartiles, whiskers represent 5% and 95% confidence intervals. **(c)** Percent of the mapped reads that can be confidently placed within a certain number of basepairs of sequencing. Note the ONT MinION sequences at approximately 450bp/sec. Only reads that were mapped by UNCALLED are considered in **b** and **c**.

Mapping a mock microbial community

Next, we tested UNCALLED's ability to map to a collection of genomes using reads from the ZymoBIOMICS High Molecular Weight DNA Mock Microbial community ("Zymo HMW") containing DNA

from seven bacterial species and one yeast (**Supplemental Table S2**). For this experiment, we analyzed 100,000 reads with an average length of 16Kbp we sequenced using a MinION (Full-Flowcell 1 control data). We mapped the signal data from these reads to a 41Mbp reference containing all genomes using UNCALLED, which mapped approximately six kilobases per second with 94% accuracy compared to minimap2 alignments of the basecalled reads (**Fig. 2a**). To test UNCALLED’s performance on different genomes, we used the minimap2 alignments to determine which reads map to each species, and then mapped each collection of reads to their corresponding reference using UNCALLED (**Supplemental Table S2**). The mean read lengths vary between ~11-21Kbp depending on the species, likely because of extraction bias, which skews the mapping rates since UNCALLED is more likely to find a confident mapping location for longer reads. When considering just reads longer than 5kbp long, UNCALLED performs similarly on all bacterial genomes. Mapping to the *S. cerevisiae* genome is ~24% slower compared to the average bacterial genome due to more repetitive sequence than the other references. However, using two iterations of the k-mer masking method described below restores the mapping speed (**Construction and Masking of a Cancer Gene Panel Reference**).

Bacterial genome depletion

Our first ReadUntil experiment was bacterial genome depletion on the Zymo HMW sample. Here, we used UNCALLED to map signal data to a 29Mbp reference containing all seven bacteria and ejected any reads that mapped within the first ten seconds of signal, with the goal of enriching the yeast sequence which was not included in the reference database. We performed three such runs: two “Full-Flowcell” runs and one “Even/Odd” run. The full-flowcell runs each used two flowcells running in parallel: one sequencing with MinNOW running in a normal configuration as a control and one with UNCALLED mapping and ejecting reads from all channels. The flowcells were selected to be similar quality based on MinNOW’s “check flowcell” feature, and the samples were prepared side-by-side and mixed prior to loading. The even/odd run used a single flowcell, where UNCALLED only monitored the even numbered channels and the odd channels were used as a control. This type of control has been used in previous ReadUntil applications^{11,14}. Once each run finished, all reads were basecalled with guppy and mapped to a reference containing all Zymo genomes with minimap2 in order to classify reads as originating from yeast or bacteria (**Fig. 2b**). Note that we classified reads that were not mapped by minimap2 as non-yeast reads, which may underestimate the on-target yield. All UNCALLED runs kept over 99% of yeast reads and ejected between 90% and 96% of bacterial reads, 75% of which mapped within the first second. The absolute enrichment of yeast sequence for these experiments ranged from 3.19 to 4.46 fold (**Supplemental Table S3**).

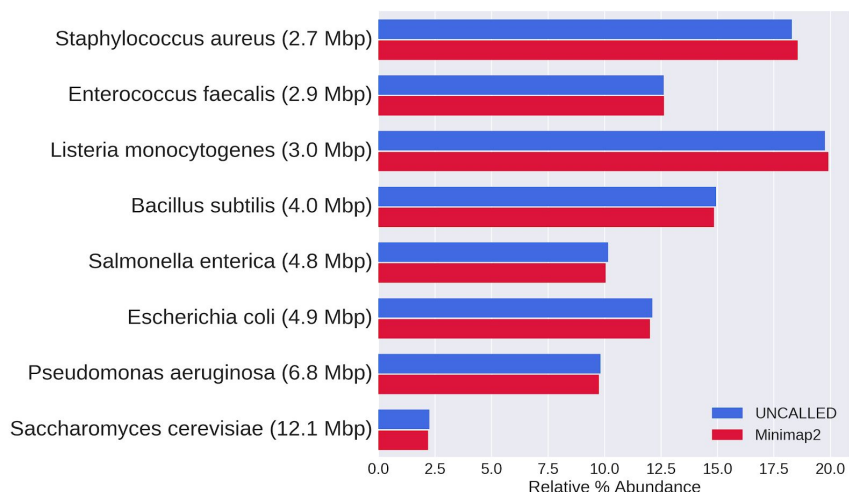
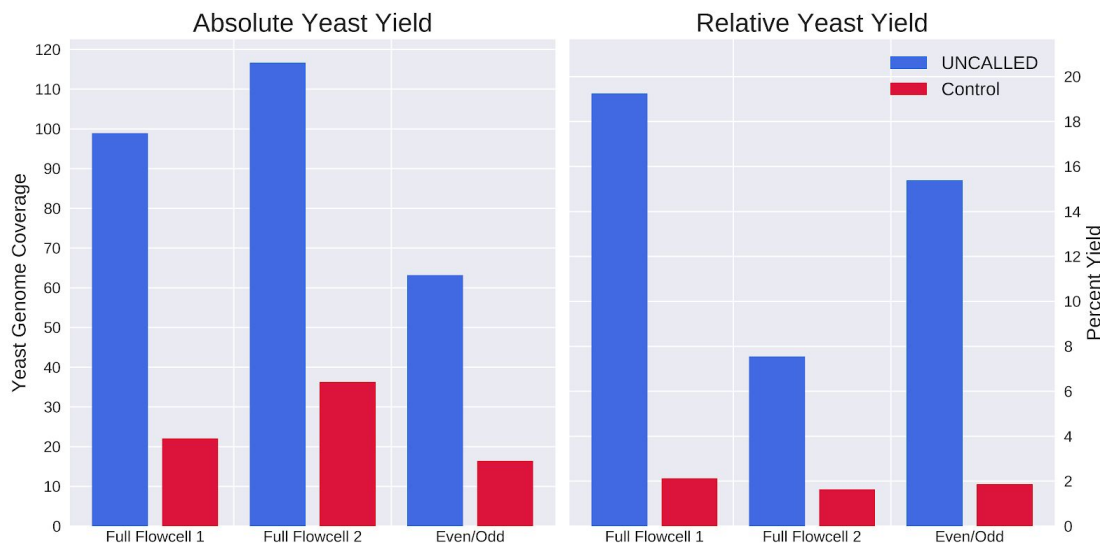
a.**b.**

Figure 2. UNCALLED results on the Zymo mock microbial community **(a)** Barchart of the relative abundances of each genome based on mapping reads from a control run to all references using UNCALLED and minimap2. **(b)** Results of UNCALLED ReadUntil depletion of bacterial genomes in order to enrich yeast sequences, including (left) a barplot of the coverage of the yeast genome in the UNCALLED and control runs, and (right) a barplot of the percent of the yield from the yeast genome in the UNCALLED and control runs.

The enrichment of the even/odd run falls between that of the two full-flowcell runs, implying that this control accurately estimates the enrichment of a full flowcell. Many factors contribute to the variability in the enrichment between runs, including read lengths, reduction in ReadUntil yield, and delayed ejections. In particular, the Full-Flowcell 2 control run had approximately half of the average bacteria read length of the control Full-Flowcell 1 run, which was a major source of the enrichment difference between these runs (**Supplemental Table S3**). We also noted that not all ejections occur as soon as the ReadUntil API request is sent, particularly on high-yield runs. In the Full-Flowcell 1 and Even/Odd runs most reads are ejected within one second of the API call, while in the Full-Flowcell 2 run most

ejections are delayed by more than four seconds, increasing the amount of off-target DNA sequenced (**Supplemental Table S3**). Ejections are more delayed early in each run when more pores are alive and actively sequencing. This suggests the ejections may be delayed when too **many** API calls are made at the same time, or when the sequencer is generally overloaded when many reads are being sequenced at once.

It is worth noting that although the on-target yield is consistently higher in the UNCALLED runs compared to the controls, the overall UNCALLED yield is reduced to between 44% and 69% of the overall control yield (**Supplemental Table S3**). Some of this reduced yield can be explained by the short period of time that a pore is empty between sequencing two reads. This gap is not significantly longer when a read is ejected compared to when it finishes normally, but the large number of ejections increases the amount of time that each pore is empty. In the Full-Flowcell 1 experiment, the average channel in the control run was empty ~20% of the time, compared to the average UNCALLED channel which was empty ~32% of the time (excluding time after channels produce their final read and between mux changes). These short gaps are unavoidable, but they do not fully explain the reduced ReadUntil yield. Inspection of the minute-by-minute channel activity throughout sequencing (duty time) shows that the number of functional channels reduces faster in ReadUntil runs, however the long-term lifetime of channels is not shorter than the control, suggesting that pores are temporarily becoming inactive (**Supplemental Fig. S3**). One potential explanation is that ejections cause more pore blockages which make pores unable to sequence reads for extended periods of time. This could be caused by single-stranded DNA on the trans side of the pore self-binding and “clogging” pores, or simply because a larger number of reads are sequenced which increases the chances that a pore will be blocked. Such blockages could possibly be cleared with a nuclease flush, which has been shown to improve yield for other ONT human genome sequencing projects (also see below)¹⁹.

Construction and Masking of a Cancer Gene Panel Reference

We next tested UNCALLED’s ability to map to a large collection of human genetic loci. For this, we evaluated an 18.6Mbp subset of the human genome containing 148 genes associated with hereditary cancer from the Invitae cancer panels²⁰. These panels consist of curated sets of genes with variants known to increase the risk of developing cancer and are widely used for clinical assessment of disease risk. Our 148 gene panel includes all primary and preliminary-evidence genes from every available organ system panel (**Supplemental Table S4**). This reference was built by extracting all exons, introns, and 20Kbp of intergenic flanking sequence upstream and downstream of each gene from GRCh38 (40Kbp of flanking sequence total). The flanking sequence was included so that reads which start outside but could extend into a gene would be mapped, and so that nearby regulatory elements such as promoters could be covered. To estimate the accuracy mapping to this reference, we used

minimap2 to map all 15.7 million reads (mean read length=8,484bp) from the nanopore WGS consortium release 6²¹ to GRCh38 and identified reads that substantially overlap with at least 94% identity any of the 148 genes. We then mapped these reads to the 148 gene reference using UNCALLED to estimate the true positive (TP) rate, which was ~81.71%, substantially lower compared to the bacterial references shown thus far (**Supplemental Table S2**). We also mapped 200,000 random reads from the WGS consortium excluding the TP reads to estimate the false positive (FP) rate, which was ~1.14%.

We hypothesized that the TP rate was reduced in the 148 gene reference was because the human genome contains much more repetitive and low-complexity sequence than bacterial references, meaning UNCALLED must consider many k-mers for certain signals and therefore uses stricter probability thresholds which make it less likely to find matching seeds. In an attempt to alleviate this we masked the most common 10-mers within the 148 gene reference using an iterative process developed for UNCALLED (see **Methods**). Using 30 iterations of this k-mer masking process raised the TP rate to a level greater than any bacterial reference, however it also raised the FP rate higher than any bacterial reference (**Supplemental Table S5**). Close inspection of these FP reads revealed that they originated from sequences in the 148 gene reference that also occur elsewhere in the human genome. We therefore developed a secondary masking procedure which masked exact repeats greater than 50bp long which occur at least five times in the human genome (see **Methods**). This reduced the FP rate to 1.52% and achieved a 91.60% TP rate, comparable to our bacterial results (**Supplemental Table S5**).

We noted that the first k-mers masked out in the iterative masking procedure were homopolymers, namely poly-A and poly-T, and that many of the subsequent k-mers masked out were simple tandem repeats. We therefore also attempted only masking such sequences to see if a simpler procedure could be used. Two strategies were attempted: first, we masked out the homopolymers running longer than 10bp in the reference sequence and then ran external masking; second, we masked out both homopolymers and tandem repeats at least 10 bp long and ran the same external masking. Tandem repeats and homopolymers are found by running MUMmer's 'exact-tandems' method ²². The true positive rates were lower for both strategies in comparison to internal iterative masking and external masking, achieving 94.31% and 94.49% for homopolymer and homopolymer plus tandem repeats respectively, whereas the iterative strategy achieves a 95.75% true positive rate. For false positive measurement, iterative masking again outperforms the two other methods, achieving 1.36% in comparison to 2.07% and 2.01% for homopolymer masking and homopolymer plus tandem repeat masking respectively. Based on these measures, we considered iterative masking to be the more effective approach.

Cancer Gene Panel Enrichment

With the mapping accuracy established, we next used UNCALLED to enrich for these cancer genes during a MinION sequencing run of the widely used GM12878 cell line. During this analysis, we used the 148 gene reference with 30 iterations of k-mer masking and external repeat masking described above. During this run, we ejected all reads that *did not* map to the gene panel within the first three seconds on one flowcell and used a second full-flowcell as control. We hypothesized that nuclease flushes could unblock pores that may be “clogged” after an attempted ejection, which could be a substantial source of reduced UNCALLED yield as previously discussed. So, we performed nuclease flushes on both runs after 24 and 48 hours and ran each for 72 hours total. The first run resulted in an average coverage over all target regions of 4.0x for the control and 14.3x for UNCALLED, for an overall 3.6 fold enrichment (**Fig. 3a**). Like previous runs, these libraries were prepared without shearing, which typically results in longer reads but reduces overall throughput. We next performed the same experiment but with shearing to 30Kbp, which resulted in an average coverage over all target genes of 5.4x for the control and 29.6x for UNCALLED, for an overall enrichment of 5.5 fold (**Fig. 3a**). In the sheared run, the minimum per-base coverage over all targeted genes for UNCALLED is 7x and over 99.9% of bases have at least 10x coverage, while genes in the control run have several regions with zero coverage and 95.1% of bases have less than 10x coverage (**Fig. 3b**). We noted that after a nuclease flush the fraction of active pores increased in both the UNCALLED and control runs, though the UNCALLED run benefitted more substantially from the flush, supporting the theory that ejected DNA causes pore blockages (**Supplemental Fig. S4**).

We next explored applications for the 29.6x coverage sheared UNCALLED reads. We first called single nucleotide polymorphisms (SNPs) and small insertions and deletions (indels) using Clair²³ on the UNCALLED and control data. For comparison, we also ran Clair on a set of reads with 51.1x coverage over the 148 genes created by combining the two GM12878 control runs, a run sequenced with the same protocol as the GM12878 sheared control, and 37.6x coverage from whole-genome sequencing (WGS) consortium. We compared each call set to the Genome in a Bottle (GIAB) NA12878 small variant truth set²⁴ using rtg-tools to compute accuracy metrics²⁵. Based on previous work^{23,26}, low-complexity regions that are known to substantially reduce small variant calling accuracy were excluded. The precision, recall, and F1 scores of the UNCALLED SNP and indel calls were within one percent of the high-coverage WGS run. In contrast, the control data had less than half the precision, recall, and F1 score (**Table 1a**). The accuracy of indel calls was lower than the accuracy of SNP calls for all datasets, which is consistent with the error profile of ONT reads as shown in previous work²³.

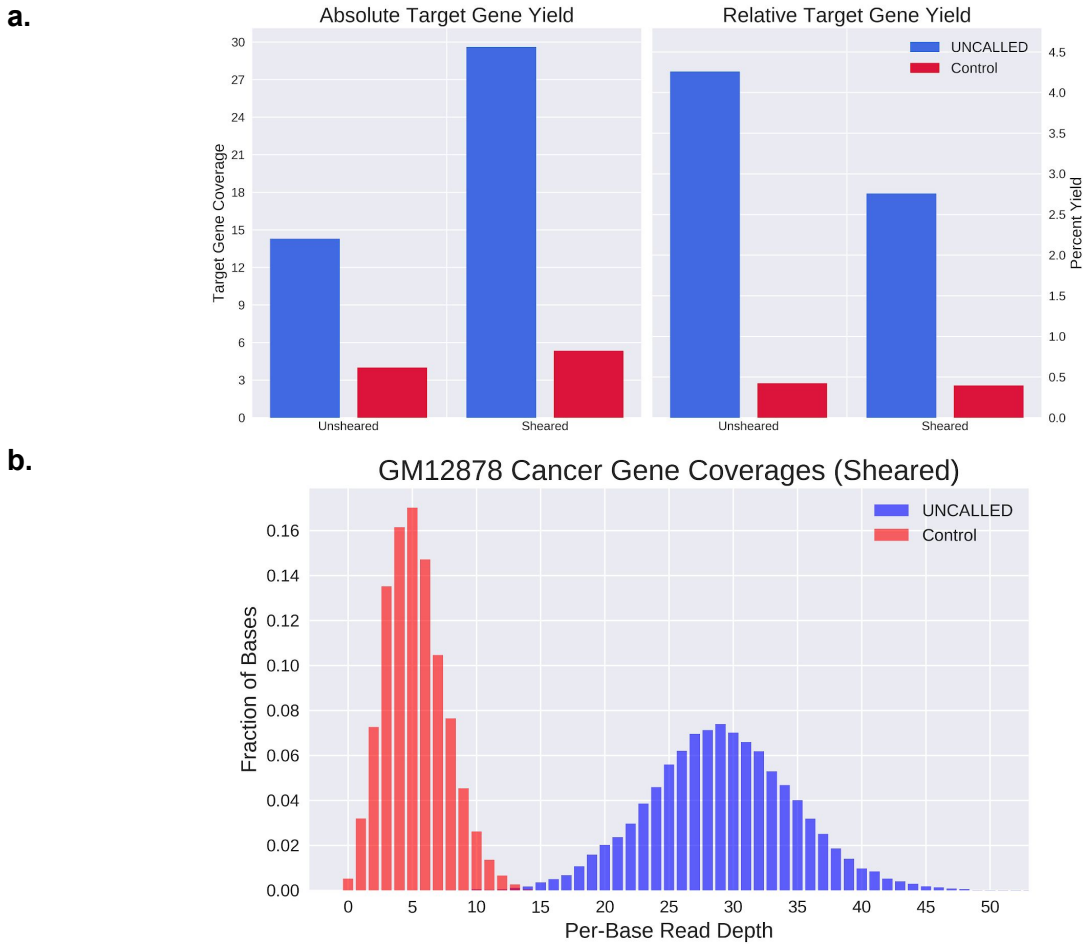


Figure 3. Human cancer gene enrichment using UNCALLED. **(a, left)** Barplot of the coverage over all 148 target genes in the UNCALLED and control runs. **(a, right)**. Barplot of the percent of the yield from the target genes in the UNCALLED and control runs. **(b)** Distribution of per-base coverage over every nucleotide in the target genes in the sheared UNCALLED run. Control ranges from 0x to 15x coverage, while UNCALLED ranges from 7x to 57x coverage.

With the small variant accuracy established we next called structural variants (SVs) at least 50bp in length in all 148 genes. The 5.4x control run has insufficient coverage for SV calling⁷, so for comparison we detected SVs using the 51.1x coverage ONT WGS run described above, 30x coverage PacBio HiFi reads, and 50x coverage Illumina reads. The PacBio and Illumina datasets were obtained from GIAB. All long-read technologies (UNCALLED, ONT WGS, and PacBio) were called using Sniffles⁷ with minimap2¹⁷ alignments and the Illumina reads were called using Manta²⁷ with BWA²⁸ alignments. Strict parameters were used for each dataset to generate sets of high-confidence SVs (**Methods**). These results were compared using SURVIVOR²⁹, which showed strong agreement between UNCALLED and ONT WGS SVs ($F1=0.94$) and between UNCALLED and PacBio SVs ($F1=0.93$), in contrast to Illumina SVs which matched fewer than half of those predicted by each long-read technology (**Table 1b**).

a.	Dataset	Count	Precision	Recall	F1
SNPs	Control (5x)	77,346	41.9%	39.4%	0.406
	UNCALLED (29.6x)	12,368	92.8%	97.6%	0.951
	ONT WGS (51.1x)	11,825	93.2%	98.5%	0.958
Indels	Control (5x)	25,070	37.6%	23.4%	0.288
	UNCALLED (29.6x)	9,844	80.4%	73.1%	0.766
	ONT WGS (51.1x)	10,374	79.9%	72.7%	0.761

b.		Total SV Count	Insertions				Deletions			
			Count	Length (bp)			Count	Length (bp)		
				Mean	Stdv	Max		Mean	Stdv	Min
UNCALLED (29.6x)	Confident SVs	50	36	196.9	175.5	974	14	-226.1	202.8	-824
ONT WGS (51.1x)	Confident SVs	50	35	206.2	178.8	964	15	-225.7	210.0	-889
	Matching UNCALLED	47	34	210.1	179.9	964	13	-241.5	220.6	-889
	Concordant UNCALLED	53	37	197.9	177.2	964	17	-206.0	204.1	-889
PacBio HiFi (30x)	Confident SVs	53	37	199.9	176.4	992	16	-173.3	107.5	-342
	Matching UNCALLED	48	34	212.4	178.8	992	14	-181.3	110.4	-342
	Concordant UNCALLED	55	39	203.3	175.5	992	16	-173.3	107.5	-342
Illumina (50x)	Confident SVs	25*	13	135.6	102.3	445	10	-159.5	111.3	-340
	Matching UNCALLED	22	13	135.6	102.3	445	7	-174.6	115.0	-340
	Concordant UNCALLED	25	14	128.2	102.1	445	9	-351.2	584.7	-1884

Table 1. Variant calling results over the 148 genes associated with hereditary cancer enriched by UNCALLED. **(a)** Accuracy metrics of single nucleotide polymorphisms (SNPs) and small insertions and deletions (indels) called by Clair. UNCALLED is the 29.6x coverage sheared GM12878 UNCALLED run, and Control is the 5.4x coverage matched control run. ONT WGS is a 51.1x coverage nanopore dataset consisting of WGS consortium reads plus three additional flowcells. **(b)** Structural variants (SV) at least 50bp in length called using the same UNCALLED and ONT WGS reads, plus 30x coverage PacBio HiFi reads and 50x coverage Illumina reads from Genome in a Bottle (GIAB). “Matching UNCALLED” only includes high-confidence SVs detected by each tool. Concordant matching allows an SV to be supported with more sensitive parameters (see **Methods**). (*) Two Illumina high-confidence SVs were inversions, so were not counted among insertions or deletions. However, they overlapped repeats and were not supported by any long-reads, so are likely false positives (**Supplemental Table S6**).

Inspection of high-confidence SVs not matched by SURVIVOR revealed that they all occur in repetitive regions, making it difficult to align short-reads and causing the reported size and location of the SVs vary slightly between the long-reads (**Supplemental Fig. S5 a-e**). Consequently, the apparent disagreements between the long-read call sets were all due to thresholding effects, such as one insertion reported to be 53bp long by PacBio reads (and thus reported as an SV) versus the UNCALLED reads which represented the insertion as 47bp (and thus not reported, **Supplemental Fig. S5a**), while the short-read calls are more fundamentally limited by the challenge of aligning short-reads to repetitive regions. To address the thresholding effects we generated SV calls from each dataset using more sensitive criteria (**Methods**). The SVs in the long-read sensitive calls sets contained matches for every previously unmatched high-confidence long-read SV, demonstrating 100% concordance between all long-read datasets (**Table 1b**). A total of 56 high-confidence SVs were identified between all long-read technologies (39 insertions, 17 deletions). The sensitive short-read calls resulted in three more concordant SVs compared to strict matching, but still only identified 45% of the SVs detected by long-reads. Four high-confidence Illumina SVs had no support from any long-read technology (two deletions, two inversions), all of which overlap annotated repeats that likely disrupt alignment of the short-reads (**Supplemental Table S6, Supplemental Fig. S5e**).

In order to characterize SVs identified by UNCALLED, we checked for overlap with or similarity to annotated repeats based on RepeatMasker³⁰ and simple repeat³¹ annotations from the UCSC genome browser³². Insert sequences extracted from PacBio HiFi reads were aligned to the human genome and the primary alignments were checked for overlap with the repeat annotations, which identified repeats in all but one of the 39 insertions (**Supplemental Table S6**). Similarly, all but two of the 17 deletion coordinates overlapped an annotated repeat. Twenty two of the insertions (~56%) and 7 deletions (~41%) were identified as general simple repeats or low-complexity sequences (e.g. "(AT)n" or "G-rich"). Nine insertions (~16%) align to an Alu element, and 5 deletions (~29%) occurred in an Alu element. Interestingly, one of these Alu insertions is located in an exon of the MUTYH gene, an important DNA repair gene associated with colorectal and breast cancers³³ (**Fig. 4**). The length is consistent with other Alu elements³⁴ and it was identified as a heterozygous insertion by all long read technologies but was not detected by the Illumina data. All other SVs occurred in intronic regions.



Figure 4. IGV visualization of a heterozygous Alu insertion in an exon of the MUTYH gene detected by UNCALLED, ONT WGS, and PacBio HiFi reads. This was not detected by Illumina reads, likely because short reads cannot span the length of the Alu repeat.

As previously discussed, nanopore sequencing is sensitive to nucleotide modifications, and UNCALLED gives us the depth to characterize them. To demonstrate this we assessed the ability to call methylation over the enriched regions using the UNCALLED sheared run with Nanopolish³, again comparing to the 51.1x coverage ONT WGS run described above. Average methylation levels were calculated for 307 annotated promoters with at least 20 CpG sites within the targeted regions for both datasets, resulting in a strong linear correlation (Pearson's=.96) (Fig. 5a). These promoter methylation levels were also compared to those called in WGBS data of two biological replicates (WGBS1 and WGBS2), also resulting in linear correlations (Pearson's WGBS1 = .85, Pearson's WGBS2 = .90). The correlation between the two WGBS replicates is also linear (Pearson's=.92). We noted one region near the transcription start site of FANCB, a gene on the X chromosome, where approximately half the reads showed hypermethylation and the other half showed hypomethylation (Fig. 5b). This pattern is likely a result of X-inactivation³⁵, where the differences correspond to maternal and paternal haplotypes.

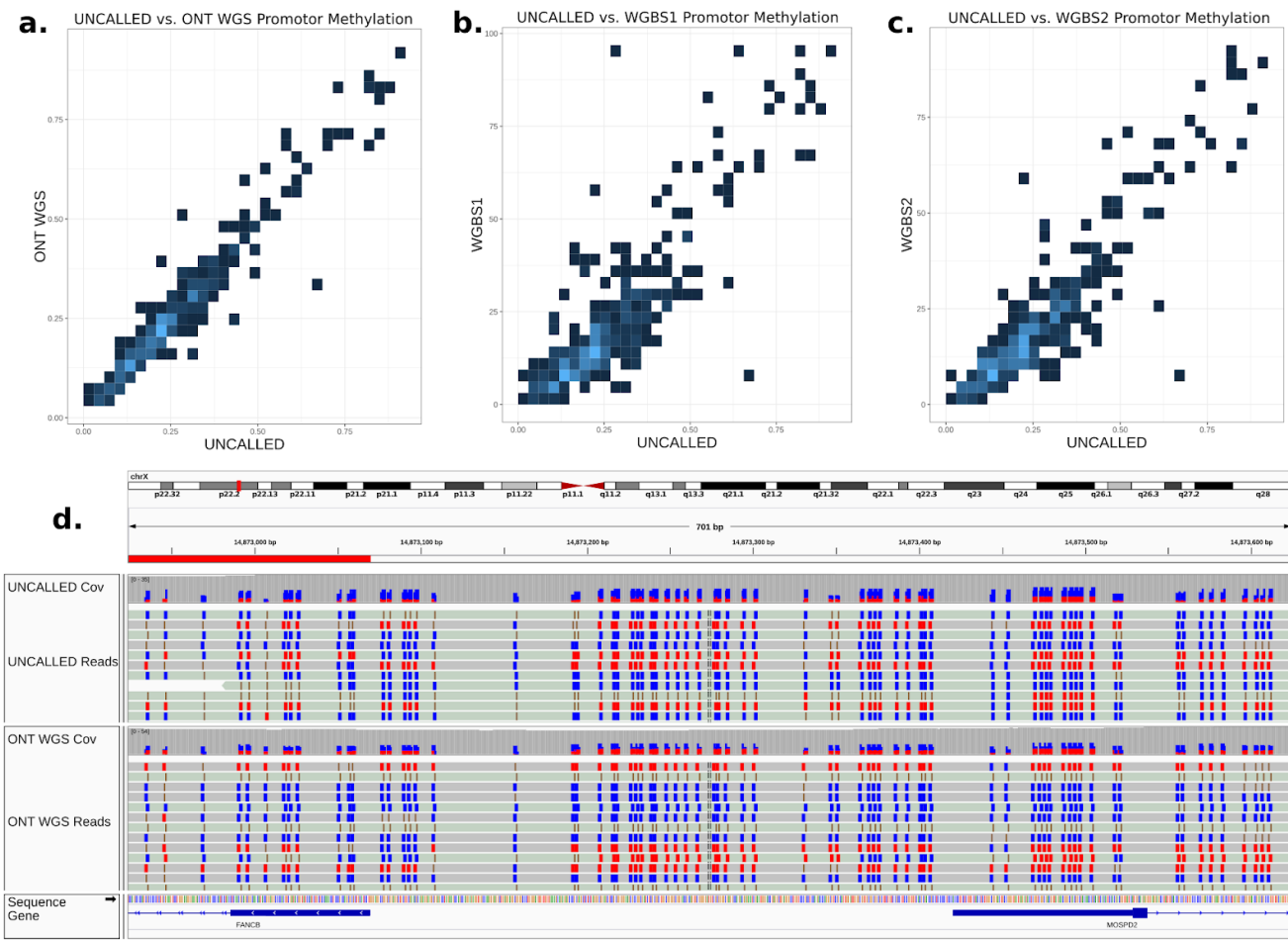


Figure 5. (a) Heatmap showing the estimated level of methylation in promoters across the targeted 148 gene regions associated with hereditary cancer in the 29.6x coverage sheared GM12878 UNCALLED run versus a 51.1x whole-genome sequencing (WGS) ONT run. (b,c) Comparison between UNCALLED promoter methylation estimates and two GM12828 whole-genome bisulfite sequencing (WGBS) runs. (d) IGV visualization at the transcription start site of FANCB on chromosome X. Each individual read tends to be fully methylated or fully non-methylated, likely due to X inactivation. Blue boxes indicate hypomethylated CpG sites, red boxes indicate hypermethylated CpG sites.

Simulating ReadUntil

Many factors affect how much enrichment is possible with UNCALLED, including read lengths, sample composition, channel occupancy, ejection delays, and mapping speed/accuracy on the particular reference. These factors interact in complex ways. For example, the mapping speed may change depending on the number of reads that UNCALLED must map at a given time, which depends on the percent of on-target reads in the sample and how many channels are actively sequencing. The number of active channels is itself affected by how many reads are ejected, which also depends on sample composition and UNCALLED's speed and accuracy. In order to model these factors, we developed a

detailed ReadUntil simulator that can be used to predict how much enrichment could be achieved on a given reference and sample.

This simulator requires two nanopore runs as input: one UNCALLED run which it uses to determine the channel occupancy “pattern”, and one (non-ReadUntil) control run to use for the actual raw electrical signal data for the reads encoded in fast5 format (**Supplemental Fig. S6, S7a**). This allows the simulator to output signal data from full-length control reads while still capturing the pore occupancy patterns of an UNCALLED run, which are different due to pore blockages and changes in electrochemistry caused by ejections. The simulator mimics the ReadUntil API, so that it can be used with UNCALLED without any modification to the underlying algorithm. It can also make accurate predictions in less time than a full 24-72 hour sequencing run by scaling down the durations of the long-term channel activity, while preserving the short-term timings of the signal and gaps between reads (**Supplemental Fig. S7b**). Importantly, in this mode the signal data is emitted at the nominal rate (1 chunk per second) but the duration between mux scans is truncated according to the desired acceleration factor.

To establish the accuracy of the simulator, we re-created two full-length runs described above: the Zymo Full Flowcell 1 bacterial depletion run, and the Sheared Human Invitae Cancer Panel enrichment run. Both simulations used the corresponding UNCALLED and control datasets as input, and were run in real-time taking 48 and 72 hours respectively (**Supplemental Table S7**). The Zymo simulation predicted an absolute enrichment of 4.43 fold (-1.12% error) and a relative enrichment of 8.99 fold (1.06% error). The human simulation predicted an absolute enrichment of 5.31 fold (-4.32% error) and a relative enrichment of 7.14 fold (2.33% error). These errors are well within the bounds seen between real runs under similar conditions (**Fig. 2**). Next, we simulated the first 24 hours of each run with varying speeds of 1x (24 hours), 4x (6 hours), 8x (3 hours), and 16x (1.5 hours). At 1x to 8x speed the estimated absolute enrichment for both runs within 0.63-2.70% of the real run, and the estimated relative enrichment was within 2.38-4.99%. Both estimates at 16x speed for the human run had over 7% error, suggesting that 1.5 hours is not sufficient time to simulate a 24 hour run, and thus all subsequent simulations were run at 8x speed using the first 24 hours of the sheared human Invitae enrichment run as a template.

With its accuracy established, we next used the simulator to predict UNCALLED’s ability to target larger sets of genes across the human genome. We first simulated targeting 717 genes from the Catalogue of Somatic Mutations in Cancer (COSMIC)³⁶ using the same gene list and coordinates as in Payne *et al.*¹⁵. Targeting all genes including introns, using 20Kbp of flanking sequence (111.44Mbp reference), and using the same masking procedure as the Invitae runs resulted in an absolute enrichment of 3.99 fold

(**Supplemental Table S8**). Assuming this enrichment level remained constant for a full 72 hours with two nuclease flushes and similar conditions to the sheared Invitae run, this would result in a mean coverage of 21.2x over all genes. However, we noted in the real sheared Invitae run the overall enrichment increased after the first 24 hours (**Supplemental Table S7**), likely because the pore occupancy was lower which reduced the CPU load. Assuming there was a proportional increase in enrichment in a 72 hour COSMIC run, we expect 24.9x coverage over all genes. We next tried enriching the same set of genes using 5Kbp of flanking sequence (89.93Mbp reference) instead of 20Kbp, which resulted in an absolute enrichment of 4.02 fold. This difference between using 5Kbp versus 20Kbp of flanking sequence is well within the previously established margin of error. Similar results were found when using 5Kbp of flanking sequence for an Invitae panel simulation

(**Supplemental Table S8**). Finally, we attempted using 20 and 40 iterations of k-mer masking on the 5Kbp flanked COSMIC reference, which resulted in absolute enrichments of 4.00 and 4.01 respectively. Again, this is not substantially different from the enrichment seen using 30 iterations, suggesting that **UNCALLED** is robust to changes in the exact number of masking iterations used or the amount of flanking sequence included.

Rather than enriching for entire genes, including introns, we next explored targeting only exons. We built references containing all exons plus 5Kbp of flanking sequence from the Invitae (9.86Mbp reference) and COSMIC (48.19Mbp reference) gene panels and performed enrichment simulations on each. The simulator predicted an absolute enrichment of 5.22 fold for Invitae and 5.23 fold for COSMIC

(**Supplemental Table S8**). It is notable how similar these levels of enrichment are despite the substantially different reference sizes, which suggests that **UNCALLED** does not have difficulty enriching for the genic sequences of this size. To test the extent of this, we built progressively larger references by extracting genes from whole chromosomes, combining chromosomes in order of how many genes each one contains (*i.e.* the smallest reference contains only chr21, the next adds chr18 and chr22, etc. See **Supplemental Table S8**). The Y chromosome was excluded because it is absent from GM12878. We created two versions of each gene collection: one with only exons, and one including introns. All used 5Kbp of flanking sequencing and 30 k-mer masking iterations. Enrichment levels were computed based on exon coverage for the exon-only references and whole-gene coverage for the whole-gene references. The absolute enrichment levels for the exon-only references ranged from 5.22 for just chromosome 21 to 3.16 for the full human exome, while the whole-gene references ranged from 4.41 to 1.66 fold enrichment (**Supplemental Figure S8**). Interestingly, the whole-gene references produce lower levels of enrichment compared to exon-only references of similar length (**Supplemental Figure S8b**), despite having very similar true positive **UNCALLED** mapping rates (**Supplemental Figure S8d**). This is because the exons comprise a much smaller fraction of the

genome than the full genes, meaning there is a larger potential for enrichment in the exon targets. The largest exon-only panel targets only 3.3% of the genome, meaning it could theoretically be enriched by a maximum of 30.03 fold, while the full gene panel targets 42.6% of the genome, meaning it could be at most enriched by 2.35 fold (**Supplemental Table S8**). Note that the target size is different from the reference size due to flanking sequence. Considering this, the 1.66 enrichment of every full gene in the human genome is not insignificant, especially since fundamentally some portion of each read must be sequenced for ReadUntil to operate.

Discussion

UNCALLED is a streaming nanopore signal mapper that can accurately map thousands of basepairs worth of signal per second to a reference millions of nucleotides in length. We have demonstrated two ReadUntil approaches: depletion and enrichment. With depletion any reads that confidently map to the reference are ejected. This analysis benefits from UNCALLED's streaming algorithm, as it does not require a fixed amount of signal to be predefined, and the read can be mapped and hence ejected at any point during sequencing. A use case for depletion, shown by our Zymo community analysis, is to deplete any known bacterial and/or viral contaminants in a sequencing run. Other applications include depleting high copy organelles or plasmids from a sample or depleting the host genome from a host-pathogen sequencing experiment. With enrichment, any reads that *do not* map to the reference are ejected. Here UNCALLED's ability to map over 90% of reads given less than 3s (~1.3Kbp) worth of signal allows us to accurately make decisions before much of the read has been sequenced. We have demonstrated an important application for this by enriching all 148 genes used in Invitae hereditary cancer panels to a depth of 29.6x using a single MinION flowcell sequencing GM12878. These data enabled SNP and indel calling more than twice as sensitive and precise as the matched control, and methylation calling that closely matched a 51.1x coverage WGS ONT run. We were also able to accurately identify 56 SVs across all 148 genes with 100% concordance compared to a high-coverage ONT WGS dataset and 30x PacBio HiFi reads, more than twice the number identified with 50x Illumina coverage. More specialized tools could increase the number of SVs detected from the Illumina reads, such as MELT³⁷ and Tangram³⁸ which are designed to find mobile element insertions, however these tools would not aid in the detection of non-mobile element SVs which comprise the majority of those identified in the Invitae panel.

Most SVs detected in GM12878 with the UNCALLED enriched reads were located in intronic regions. While these certainly could have functional effects, exonic mutations are more likely to disrupt gene activity. A single heterozygous insertion was located in an exon of the MUTYH gene (**Fig. 4**), which is a gene involved in DNA repair³³. Homozygous mutations in this gene are known to cause adenomatous

colorectal polyposis, a disease that highly increases the risk of developing colorectal cancer³⁹, and there is some evidence that heterozygous mutations also increase this risk⁴⁰. Additional analyses and/or functional validation are necessary to determine the effect of this insertion, but a result such as this in a patient would indicate that the individual could be a carrier for adenomatous colorectal polyposis, and could themselves be at a higher risk of developing colorectal cancer.

To further benchmark UNCALLED, we also developed a ReadUntil simulator which allowed us to predict how much UNCALLED could enrich using various target references. This strongly demonstrates the potential for UNCALLED to target all 717 COSMIC genes or even the whole human exome, albeit at modestly lower levels of enrichment than the smaller Invitae panel. The simulation of the human exome run suggests that a 72 hour run with two nuclease flushes could reach a mean coverage of 14.1-16.5x of the exome. The simulations demonstrated interesting properties of ReadUntil, especially the intrinsic limitation of enriching for larger proportions of DNA in the sample. It is important to note that these simulations assume identical sequencing conditions as the sheared Invitae enrichment run, which was used as a template. Changes to the read length distribution or flowcell quality, would also change the results. It is also possible that factors such as ejection delays or pore blockages could also change when target sequence is changed. More experiments are required to model these effects. Regardless, this simulator will be a valuable resource to predict enrichment levels before committing to a real sequencing run of any genome and sequencing target.

We have noted several technical issues with the ReadUntil method including read length dependence, pore blockages, and delayed ejections. While UNCALLED is generally more effective with longer reads, longer reads are also associated with lower yield, meaning these factors must be balanced to maximize the on-target yield. This is exemplified in the unsheared and sheared human gene enrichment runs, where the sheared UNCALLED run has a lower percent of on-target yield than the unsheared run, but the absolute on-target yield is higher (**Fig. 3a**). Both ONT yield and read lengths have continually improved historically, so the dependence on long reads is likely to be less of a limitation in the future. Pore blockages are largely eliminated with nuclease flushes, but this requires additional input DNA and preparation time. Blockages could possibly be alleviated by adjusting the voltage applied during ejection, or be avoided by not ejecting reads that map near certain motifs that are likely to self-bind and cause a blockage. ONT has also recently announced plans to incorporate nuclease enzymes directly within the trans side of the pore which could make manual treatments unnecessary⁴¹. UNCALLED could also eject reads earlier if provided smaller chunks of signal. The ReadUntil API currently only provides signal in one second chunks, while UNCALLED can usually map 75% of reads in less than one second. Reducing this minimum time would allow many reads to be ejected earlier.

UNCALLED's performance degrades as references become larger and more repetitive, including when the reference is composed of a collection of many genes and/or many individual genomes. The size effect is mainly due to the increase of repetitive sequences, since the odds that any sequence appears multiple times in a reference increases with reference size. While we have demonstrated several use cases for UNCALLED, including the enrichment of 148 human genes at once and potentially the entire human exome, broadening the types of sequences that UNCALLED can enrich or deplete could be very useful. Optimizations such as further improving the cache-efficiency of the mapping procedure and utilizing SIMD instructions available on modern processors could substantially improve UNCALLED's performance on any reference. Also, while the repeat masking described here was effective, modifications to the indexing procedure and/or core algorithm could eliminate the need to mask entirely. We also intend to develop a GPU implementation of the UNCALLED algorithm, which could drastically improve the speed, especially to support PromethION sequencing that has more pores available per flowcell and can run multiple flow cells in parallel. This will allow UNCALLED to leverage the same computing power as methods which use specialized GPUs to basecall for ReadUntil¹⁵. Basecalling reads first, no matter how efficient, levies an additional computational burden requiring more powerful computers and additional time for a sufficient amount of signal to be cached, meaning delayed ejections and lower enrichment.

In the future, UNCALLED could be used for additional applications than demonstrated here with little or no modification to the algorithm. For example, UNCALLED could currently enrich or deplete cDNA sequences, which could be useful in avoiding sequencing highly abundant genes or targetting for known gene fusions. ReadUntil with direct RNA sequencing is also possible, although this would require an accurate RNA k-mer model and optimized event detection parameters to account for the different and less stable translocation speed. UNCALLED could also be used in conjunction with other enrichment methods, such as CRISPR/Cas9 enrichment. These methods produce many off-target sequences, which UNCALLED could eject to further improve the amount of on-target DNA. Lastly, UNCALLED can enable many new dynamic applications. For example, an UNCALLED index could be built on-the-fly during a metagenomics sequencing run from the most highly abundant genomes, which could then be depleted for the remainder of the run to increase the coverage for less abundant species. The dynamic nature could also be used to shift the coverage requirements for sequencing below the typical Poisson distribution by selectively ejecting reads from regions of the genome that already have sufficient coverage available. Finally, we also intend to add an optional dynamic time warping (DTW) step to UNCALLED, making it a full-scale signal-to-basepair aligner. This could aid in raw signal applications outside of ReadUntil, such as assembly polishing, identifying nucleotide modifications³,

and classifying variable number tandem repeats⁴². UNCALLED could improve the sensitivity of such analyses by eliminating the need for basecalling, which can be error prone around such features.

Acknowledgements

We would like to thank Taher Mun for his contributions on an early prototype of UNCALLED, and Timothy Gilpatrick for providing extracted GM12878 DNA used in the cancer gene enrichment experiments.

This work was funded, in part, by the US National Science Foundation (NSF) grant DBI-1350041 (MCS) and US National Institute of Health (NIH) grant 1R01HG009190 (WT). WT holds two patents currently licensed by Oxford Nanopore Technologies Limited. MCS and WT have received travel funding from Oxford Nanopore Technologies Limited.

Contributions

SK and MCS designed UNCALLED. SK implemented UNCALLED. BN and SK benchmarked UNCALLED. YF performed all sequencing library preparation. SK computed enrichment levels for all experiments and performed small variant and structural variant detection and analysis. YF performed methylation detection and analysis. WT supervised sequencing runs and advised on the experimental design. MCS supervised the entire project. All authors contributed to writing the manuscript. All authors read and approve the final manuscript.

Online Methods

UNCALLED Algorithm

The core algorithm can be split into three main stages: signal processing, seed mapping, and seed clustering.

The signal processing stage probabilistically decodes the raw signal data into the k-mers they represent. It is based on early Hidden Markov Model (HMM) basecallers, where stretches of similar signal are first collapsed into “events”, which ideally represent the same k-mer⁴³. The event detection process can make two types of mistakes, which can be classified as “stays” (multiple events that represent the same k-mer), and “skips” (one event that represents multiple k-mers). Stays are far easier to handle than skips combinatorially: if we know the k-mer associated with one event and we want to predict the next, if we assume the only errors are stays then there are up to five possible next k-mers (extend by A, C, G, or T, or stay), while including skips results in 21 possible extensions (the previous 5 plus extend by AA, AC, AG, AT, CA, etc). We therefore use event detection parameters which are tuned to typically result in ~50% stays and ~1% skips. UNCALLED’s event detector is based on open source event detection code from Scrappie (<https://github.com/nanoporetech/scrappie>), which uses t-tests over rolling windows to detect when the signal changes significantly to define event boundaries. This code was modified to operate in a streaming manner for UNCALLED. The UNCALLED version produces identical events compared to Scrappie event detection given the same signal and parameters.

Each event is represented by the mean of the signal that it covers. As events are detected, they are normalized so that the mean and standard deviation of a rolling window of events match that of the k-mer model released by ONT⁴⁴. This is accomplished with a streaming algorithm that computes the mean and variance based on the Welford algorithm⁴⁵ adapted to maintain the rolling window, allowing the normalization to adjust for drift in the signal characteristics throughout sequencing. The default normalization window is 6,000 events long to ensure a robust sampling of all possible k-mers.

After normalization, UNCALLED calculates the probability that each event matches each possible k-mer based on ONT’s k-mer model. This model lists the expected mean and standard deviation of the signal associated with each 6-mer, which is modeled as a normal distribution. To accelerate computational processing, UNCALLED uses a simplified model of 5-mers with little loss of information when computing event/k-mer match probabilities. During signal processing, UNCALLED picks a probability threshold that is dynamically altered depending on how uniquely the seed is mapping, and considers all k-mers which match each event above that threshold (see **Index Probability Thresholds** below).

The seed mapping stage attempts to find relatively short but perfect alignments between the read and the reference genome. UNCALLED uses an FM-index, which is the data structure used by many aligners such as Bowtie⁴⁶, BWA²⁸, and HISAT⁴⁷. BWA provides a library for its FM-index, which UNCALLED directly uses to take advantage of its highly optimized construction and querying. The FM-index allows one to find all locations of an arbitrarily long query sequence in a reference, with time essentially constant with respect to the reference size. UNCALLED uses a novel branching algorithm which considers all k-mers that each event can match at each step of the mapping. This algorithm speed is not constant with respect to the reference size due to the branching, but scales much better compared to dynamic time warping.

Given a new read, UNCALLED first finds all locations of all k-mers which match the first event. The FM-index allows an efficient representation of all locations of each unique sequence. For the next event, it checks if that event could match any k-mers “compatible” with any of the k-mers that matched the previous event. A 5-mer is compatible if its first four bases match the previous 5-mer’s last four bases, or if they are the same 5-mer in the case of a stay. Each compatible non-stay k-mer extends the previous sequence by one basepair, and we use the FM-index to find the locations of each extended sequence. This search space conceptually forms a forest of trees, where each possible sequence and the locations of that sequence are represented as a path from a root to a leaf (**Supplemental Fig. S1**). After existing mapping paths are extended, UNCALLED begins new paths by finding the locations of k-mers that match the event but are not represented in the previous paths. Again, the FM-index provides an efficient mechanism to accomplish this. The UNCALLED algorithm proceeds by alternating between extending old paths and creating new ones, and can report a seed mapping when one sequence narrows down to a unique location in the reference.

Storing mapping paths as nodes of trees connected by edges would be computationally intensive due to cache inefficiency when accessing non-contiguous memory. To improve performance, UNCALLED stores each path from a root to a leaf in a “path buffer” (**Supplemental Fig. S9**). Each path buffer stores cumulative log probabilities of each event matching each chosen k-mer, and other information such as the FM-index location and the most recent k-mer matched. When a path branches, the buffer is copied to preserve this information for each extension. The length of the path buffers determines the seed length, and a seed is only reported if the buffer is full and the mean probability over all events in the buffer is above a threshold. When an event is added to a full buffer, the oldest event is erased and all other events shift to make room for the new event, allowing subsequent seeds to build off of previous seeds.

The seed clustering stage separates true alignments from spurious seed matches. Due to the noisy nature of nanopore sequencing, UNCALLED must use very loose thresholds for event/k-mer matches, which produce many false positive seed mappings. We eliminate these false positives under the observation that they will usually map to random locations, while true positives will map to locations consistent with their position on the read. This analysis is complicated by stays, which can occur inconsistently: there are often long stretches of stays followed by many non-stays. We therefore developed a rapid clustering algorithm which groups seeds together if their read and reference coordinates are consistent with each other. Specifically, the distance between read coordinates of adjacent seeds must be larger than the distance between the reference coordinates, but not by more than a factor of 12 by default, which handles most stretches of “stay” events. When a seed is added to an existing cluster of seeds, we update the total number of reference basepairs that the cluster covers, which is used as a measure of support for that reference location. We report a read mapping once the ratio of the best supported location over the next best supported location is above a threshold (default: 1.85 fold), or the ratio of the best supported location over the mean support for all locations is above a different threshold (default: 6.00). The first threshold is sufficient for most non-repetitive regions, while the second threshold is somewhat more repeat tolerant.

Index Probability Thresholds

UNCALLED uses the BWA library for constructing, storing, and querying the FM index²⁸. After the index is constructed, reference-specific probability thresholds must be precomputed to maintain accuracy and speed for references of different sizes and repeat contents. These thresholds are used to decide which k-mers can be used to extend a path based on the event/k-mer match probabilities (see **the signal processing stage** above). The threshold to be used depends on how many reference locations that the path being extended could currently map to, which is determined by the length of the FM index range associated with the path buffer (FM range size, **Supplemental Fig. S2**). The goal in choosing these thresholds is to limit unnecessary branching in the seed mapping process. A path buffer that could map to many locations (a large FM range size) should use a strict threshold, meaning fewer k-mers are likely to be considered, since each location that a path can map to could form a new branch later in the mapping process (**Supplemental Fig. S1**). As a path gets longer the number of locations to which it could map tends to decrease, and so using more permissive probability thresholds for smaller FM range sizes increases the odds that events extending longer paths will correctly match the k-mers they represent. The correspondence between FM range sizes and probability thresholds must vary depending on the reference, since paths of the same length are likely to have longer FM range sizes as references become larger and more repetitive.

UNCALLED uses a different log probability threshold for every power of two FM range size, and assigns thresholds such that FM ranges with size in the range $[2^s, 2^{s+1}]$ share the same threshold for any positive integer s (**Supplemental Fig. S2b**). This works well since FM range sizes decrease exponentially as mapping progresses, and it is computationally efficient to index in real-time by computing the log base two. We developed an EM algorithm to assign probability thresholds for intervals of FM index range sizes with the goal of minimizing the total amount of time required to map a read.

Mapping paths are always extended one nucleotide at a time. It is useful to have a correspondence between the number of nucleotides mapped, which we call the “path position”, and the expected FM range size at that position. To find this correspondence we use the FM index to map the reference genome to itself from many random locations (one out of 100 genome locations by default) until a unique location is found, which provides a sampling of the FM range sizes for each path position. We then compute N , which is the number of basepairs required to map 95% of positions uniquely (by default), and M which is the maximum log FM size for all k-mers in the genome ($k = 5$ for the 5-mer model used by UNCALLED). For every $p \in [k, N]$ we compute the mean \log_2 FM range size after p basepairs are mapped which we call $F(p)$, and for every $f \in [1, M]$ we compute the mean of all path positions with FM range size f , which we call $P(f)$. These functions allow us to pick thresholds with respect to path positions and then map those thresholds back to FM range sizes. Assuming we have some function $T(p)$ which returns a log probability threshold for every path position $p \in [k, N]$, we aim to compute a “speed coefficient” S which is proportional to the basepairs per second that we expect to map. We can then use an EM algorithm to adjust $T(p)$ until an optimal S is found. S is computed based on the mean number of k-mers that we expect to match an event above each threshold, which we call $B(t)$ (**Supplemental Fig. S2a**, blue line). For each path position, the amount of work UNCALLED must perform is proportional to the number of k-mers we expect to consider at the given threshold multiplied by the number of reference locations that currently considered: $B(T(p)) \times F(p)$. These values are summed for every path position and normalized to compute S :

$$S = \frac{\sum_{p \in [k, N]} B(T(p)) \times F(p)}{\sum_{p \in [k, N]} F(p)}$$

Finally, we must define $T(p)$ to be some increasing function that has an adjustable variable to optimize with the EM algorithm. Various functions were tested, but the one used in UNCALLED is based on the power function: $y = x^\theta$. This function always intersects $(0,0)$ and $(1,1)$ making it easily scalable, and

adjusting θ makes it increase faster or slower. This requires some fixed initial and final probability threshold, which we call t_0 and t_N respectively. The default values for t_0 and t_N are -10.00 and -2.25 respectively (both natural log probabilities), which were empirically determined to be the lowest and highest useful thresholds (**Supplemental Fig. S2**). We then define $T(p)$ as:

$$T(p) = t_0 + (t_N - t_0) \times \left(\frac{p}{N}\right)^\theta$$

The EM algorithm then works by adjusting θ until S reaches the target value. The default target for S is 115, which was empirically found to minimize the total amount of time to map reads to various references. Once θ is found we can compute $T(P(f))$ for all $f \in [1, M]$ to find probability thresholds for every \log_2 FM range size. An example set of probability thresholds computed for the *E. coli* K12 reference genome can be seen in **Supplemental Fig. S2b**.

Implementation

UNCALLED is available open source at <https://github.com/skovaka/UNCALLED>. The core algorithm is written in C++, with a Python frontend to interact with the ONT ReadUntil API. UNCALLED uses the BWA²⁸ FM-index to take advantage of its highly optimized construction and querying. The BWA index was chosen because it was available as a library and is highly optimized for DNA alignment, unlike more general-purpose libraries like SDSL⁴⁸ which are designed for larger alphabets. It can be run as a standalone read mapper in addition to live ReadUntil, and outputs locations in the PAF (Pairwise mApping Format) introduced by Minimap⁴⁹. UNCALLED was run on a 24 core 3.0 GHz Intel Xeon Gold 6136. All mapping speeds were measured by running with a single thread. All ReadUntil experiments were run using 48 threads.

Zymo Bacterial Depletion Experiments

Bacterial reference genomes for the ZymoBIOMICS High Molecular Weight (HMW) DNA Standard were obtained from the ZymoBIOMICS (<https://s3.amazonaws.com/zymo-files/BioPool/D6322.refseq.zip>). A *S. cerevisiae* draft genome was also included, but this reference was highly fragmented, so the S288C reference genome (NCBI accession GCF_000146045.2) was used instead for mapping with UNCALLED and Minimap2.

The Full-Flowcell 1 UNCALLED run ejected reads throughout the entire sequencing run including during “mux scans” when the sequencer checks pore quality to prioritize pore usage. Subsequent ReadUntil runs did not eject during mux scans in an attempt to improve yield by preventing ejections that might disrupt the MinION’s ability to check pore quality. This did not appear to have a substantial

impact on ReadUntil yield, but the feature was left in to not disrupt the mux scans since they account for less than 2% of sequencing time.

Hereditary Cancer Gene Reference

The 148 genes associated with hereditary cancer were obtained from the Invitae website by extracting the names of all primary and preliminary-evidence genes from every listed panel²⁰. The coordinates of these genes in GRCh38 were identified in the Ensembl gene annotation (v98)⁵⁰. The gene coordinates were extended by 20,000bp on each end to include flanking sequence, and the sequences at those locations were extracted from GRCh38 using bedtools⁵¹ to obtain an 18.6Mbp reference.

Two forms of masking were performed on the reference containing 148 human genes. The first is an iterative process based on identifying the most common 10-mers that occur within the reference. In each iteration the most common 10-mer is first identified using jellyfish⁵², and then that k-mer is masked by replacing each occurrence with “N”s. The BWA indexing procedure replaces any “N” with a random basepair, making it highly unlikely that a read will falsely map to ten or more “N”s. In the next iteration the masked reference from the previous iteration is used, meaning the previously most common k-mer will no longer occur, and any k-mers overlapping that k-mer will have a reduced count. This method was also applied to the *S. cerevisiae* genome to demonstrate an improvement in mapping speed. **We also tested only masking homopolymers 10bp or longer, and masking all homopolymers and simple tandem repeats, all identified using MUMmer’s ‘exact-tandems’ function²² with minimum repeat length set to 10bp.**

The 10-mer masking process is effective in increasing the TP rate, but also increases false positives caused by repeats outside of the reference. To identify these external repeats we first extracted all 50bp windows from the 148 gene reference and aligned them to the full human genome using bowtie⁴⁶, using parameters which find all exact end-to-end matches (-a -v 0). We then found all windows that occur at least five times in the genome and merged them to find all contiguous regions 50bp or larger that occur at least five times. These regions were again masked by replacing them with “N”s.

Small Variant Calling

For consistency all nanopore data was basecalled using Guppy v3.2.4, including the WGS consortium data. SNPs and Indels were called using Clair²³ with the alternative allele frequency threshold set to 0.2 as recommended for ONT reads. We used the vcfeval command in rtg-tools²⁵ to compute precision, recall, and F1 scores. For the truth set we extracted all entries in the Genome in a Bottle (GIAB) NA12878 small variant truth set²⁴ which overlap the target genes, and removed variants which overlap low-complexity regions which negatively impact small variant detection benchmarking according to the

Global Alliance for Genomics and Health (GA4GH)^{23,26}. Variants in these regions were also removed from the Clair outputs. This was done based on regions specified in previous work²³.

Methylation Calling

CpG methylation was called using Nanopolish on default settings. Promoter regions, as annotated in the Ensembl regulatory features of GRCh38, within the targeted regions were identified using bedtools⁵¹. Average methylation frequency was then calculated over these promoters. WGBS CpG methylation data of GM12878 biological replicates were downloaded from the Gene Expression Omnibus (GEO) database (Accessions GSM2308632 and GSM2308633) in bed file format. For read-level visualization, CG positions and methylation calls were annotated in the alignment files (<https://github.com/isaclee/nanopore-methylation-utilities>).

Structural Variant Analysis

High-confidence long-read SVs were found using Sniffles⁷ with a minimum SV length of 50bp and a minimum read support of one quarter of the average coverage: 7 for UNCALLED and PacBio, and 13 for the high-coverage WGS dataset. All other Sniffles parameters were left at their defaults. The minimum read support was chosen to be one quarter of the average gene coverage per sample as used in other studies^{7,53}, based on the fact that heterozygous SVs should be represented in approximately half of all reads so that one quarter of reads will capture SVs with high probability⁵³. High-confidence short-read SVs were found using Manta²⁷ using the default score cutoffs. Only SVs that are less than 1Mbp in length, do not include translocations to other chromosomes, and overlap one of the 148 cancer genes were considered for both Sniffles and Manta. The high-confidence SVs were matched using “SURVIVOR merge” with a maximum distance of 1,000bp and requiring the same variant type and strands. Because of the noise in the raw ONT reads, Sniffles split the same SV into two separate SVs in both the UNCALLED and WGS datasets (**Supplemental Fig. S5f**), which SURVIVOR merged in the WGS run but not UNCALLED. Accordingly, this case was manually corrected. Matches for previously unmatched high-confidence SVs were found using more sensitive criteria in Sniffles (minimum length of 30bp, minimum read support of 3, and maximum SV grouping distance of 50bp), and using all Manta SVs regardless of scoring. The maximum matching distance in SURVIVOR was also set to 1,500bp for merging the sensitive call sets.

Deletions were characterized by first intersecting their reference coordinates with all RepeatMasker³⁰ entries downloaded from the UCSC Genome Browser³² using bedtools⁵¹. If no overlap was found with RepeatMasker, we searched for overlaps with the “Simple Repeat” track from UCSC Genome Browser, which is based on Tandem Repeat Finder annotations⁴². Insertions were classified by extracting the insert sequence output by Sniffles for the PacBio HiFi SV calls, aligning this sequence to GRCh38

using BWA MEM²⁸, and intersecting the alignments with RepeatMasker and Simple Repeats. No alignment was found for two of the insertions, so these were characterized by their reference coordinates in the same way as deletions.

ReadUntil Simulator

The ReadUntil simulator models each simulation on two real runs, taking read signal data from a control run and gaps between reads from an UNCALLED run (**Supplemental Fig. 7a**). These are parsed via the sequencing summaries output by ONT basecallers, in addition to the UNCALLED PAF file and the control fast5 files. Reads and gaps within mux scans are excluded since UNCALLED ignores chunks within them. The gaps, defined as the time between the end of one read and the start of the next in the same channel, are classified into “short” and “long” gaps using a threshold of one standard deviation over the median (**Supplemental Fig. 6**). Short gaps are dynamically placed between individual reads, and long gaps define periods where a channel is entirely inactive. Within each channel, the gaps are organized into “scan intervals”, which are defined as a period of time between two mux scans (90 minutes by default). This is because the gap durations between reads for a given channel are generally stable between mux scans, while they can drastically change between mux scans when most pore transitions occur (**Supplemental Fig. 6**). Scan intervals are synchronized across channels, meaning all channels start and end their intervals at the same time.

When a new read is produced, a short gap is sampled from the active scan interval and no chunks are output until the duration of the short gap has passed (**Supplemental Fig. 7a**). This allows the simulation to be dynamic by enabling an arbitrary number of reads to be simulated, which is necessary because a large number of ejections could provide time for more reads. Long gaps, on the other hand, are stored as static “active” and “inactive” time periods which define when a channel should and should not produce reads. In order to accelerate the simulation the active/inactive periods and scan interval lengths, but not the short gaps or read durations, can be scaled down by some constant (**Supplemental Fig. 7b**). This essentially downsamples the overall number of reads sequenced while retaining the short-term channel activity patterns, thus allowing for an accelerated run to be accurately modeled.

The simulated reads are loaded from a control run so that any read could be potentially simulated as full-length (not ejected). Only the maximum number of chunks that UNCALLED will attempt to map are loaded to limit the loading time and the amount of RAM required. For example, in the Zymo bacterial depletion simulations ten chunks are loaded for each read, while in the human gene enrichment simulations only three chunks are loaded. The full sequencing duration (in seconds) of each read is

also loaded so the simulator can spend the appropriate amount of time on each read. The channel-by-channel activity of the UNCALLED and control run are unlikely to be similar to each other, meaning channels are unlikely to produce similar numbers of reads or be active or inactive at the same times. In fact, an UNCALLED run typically produces many more reads than the control because of read ejections. Because of this, reads are associated with whole channels rather than scan intervals to avoid differences between interval activity (**Supplemental Fig. 7**).

Read counts are normalized by re-assigning reads to channels while attempting to keep reads originating from the same channel together as much as possible. This is needed to preserve similarity between signal characteristics of consecutive reads. First, UNCALLED and control channels are sorted by read count and control reads are tentatively assigned to UNCALLED channels in sorted order. We then compute the target number of control reads that should be assigned to each channel by normalizing the UNCALLED channel counts to the number of control reads, with a minimum number of reads required per channel (ten by default). Next channels are sorted by the difference between the tentative counts and target counts. Finally, reads from channels with the highest excess of reads are iteratively moved to channels with the highest deficit, moving reads in contiguous blocks to preserve signal similarity between consecutive reads.

At the start of a simulation, each channel that is active samples a short gap from its first scan interval and a read to be used as their first active reads. The short gaps precede the reads, and no chunks are output until each gap duration passes (**Supplemental Fig. 7**). After each gap, chunks are output after each chunk duration (one second) passes until no more chunks are available, after which UNCALLED does not accept more chunks. If UNCALLED requests an ejection, the read duration is shortened after an ejection delay, which is set to the median ejection delay observed within the input UNCALLED run. After the read duration passes, if the channel is still in an active period then another read and short gap are sampled and the process repeats. When all channels reach the end of their scan intervals the simulator outputs nothing for ten seconds to allow all UNCALLED mappers to reset as they do in a mux scan, then moves on to the next set of scan intervals.

After the simulation concludes, a post-processing script estimates enrichment level by examining the simulation output PAF file along with the control sequencing summary to translate sequencing durations into yield estimates. If the simulation was run at a faster speed these yield estimates are appropriately scaled to project the full-length run yields. When comparing simulated enrichment levels to real runs, we excluded reads which occurred during mux scans in the real runs because mux scans were not simulated.

The simulator was developed as part of UNCALLED version 2.0, released under the v2.0 tag on GitHub. This also included minor changes to how probability thresholds are computed for different indexes in order to handle particularly small or large indexes. The indexing procedure still follows the framework described above, but the parameters chosen, and thus the exact mapping speed/accuracy, for certain references may vary slightly between version 2.0 and version 1.0, which was used for all non-simulation experiments.

Samples

ZymoBIOMICS HMW DNA Standards were purchased from Zymo Research. GM12878 cells were purchased from Coriell Institute and propagated in Dulbecco's Modified Eagle Media (DMEM) with fetal bovine serum (FBS), penicillin, and streptomycin at 37°C and 5% CO₂. Cells were then snap frozen in pellets of roughly 2 million cells, and DNA was extracted from the cell pellets using the Nanobind Cells, Blood, Bacteria (CBB) Big DNA Kit from Circulomics according to the manufacturer's specifications. The extracted DNA was then directly sheared without dilution to 30kb using the Diagenode Megaruptor 2. Sheared samples were processed twice in a row on these settings due to the viscosity of the extracted DNA. Before library preparation, short fragments of DNA were depleted from the samples using the Circulomics Short Read Eliminator XS (SRE XS) kit, according to the manufacturer's specifications.

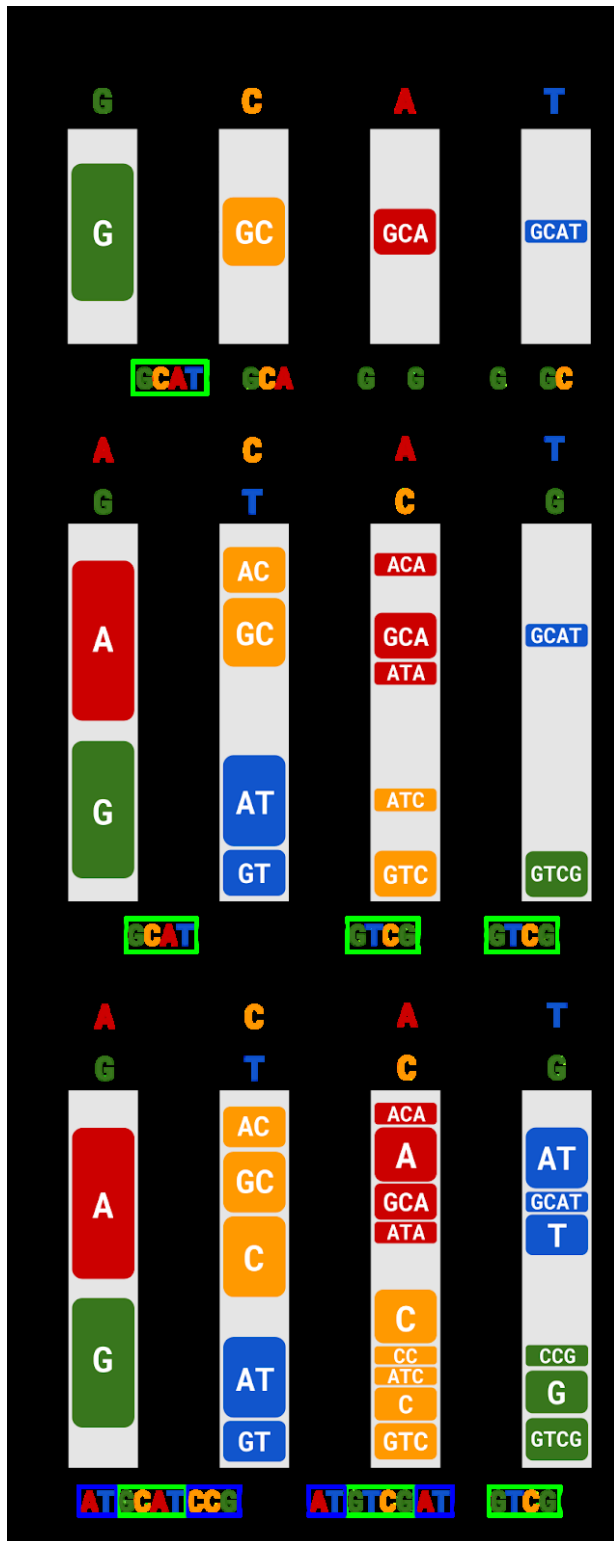
Library preparation

All sequencing libraries were prepared using the ONT Ligation Sequencing Kit (SQK-LSK109) without the DNA Control Strand (DCS) or FFPE repair in the end prep step. The initial sample volume was thusly adjusted to 50ul, and Ultra II End Prep Reaction Buffer volume was adjusted to 7ul. Nuclease flush Buffer A was prepared by combining 659ul of ultra pure water, 300 ul of 1M KCl, 30ul of pH 8.0 HEPES buffer, 10ul of 1M MgCl₂, and 1ul of 2M CaCl. Just prior to loading the flowcells, the libraries for the control run and the UNCALLED run were mixed together, as were the priming buffers for the runs. ONT MinION flowcells (FLO-MIN106) with vR9.4.1 pores were used for all sequencing. Flowcells were selected such that the estimated available pores on the UNCALLED and control runs were within 200 pores of each other (out of ~1,400 to ~1,700 total pores). The runs used in addition to the WGS consortium data for the high-coverage WGS SV calls were the two GM12878 control runs, plus another library sequenced with the same protocol as the unsheared GM12878 control run.

Data Availability

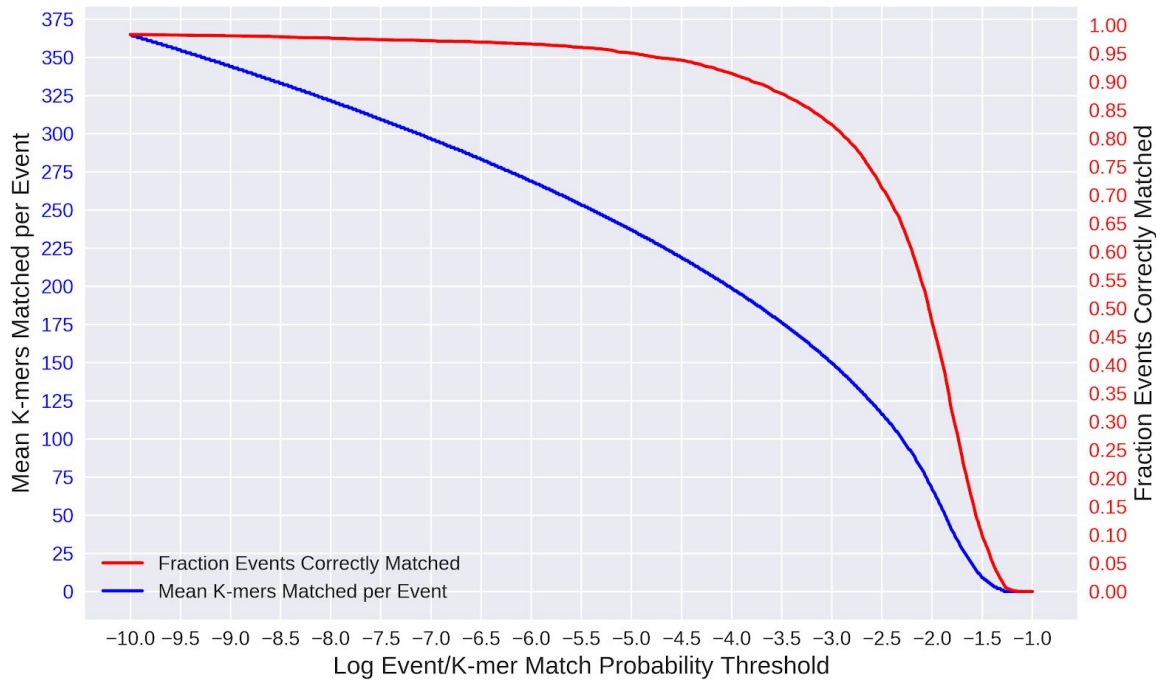
All sequencing runs are available as an NCBI BioProject under the accession PRJNA604456.

Supplemental Figures

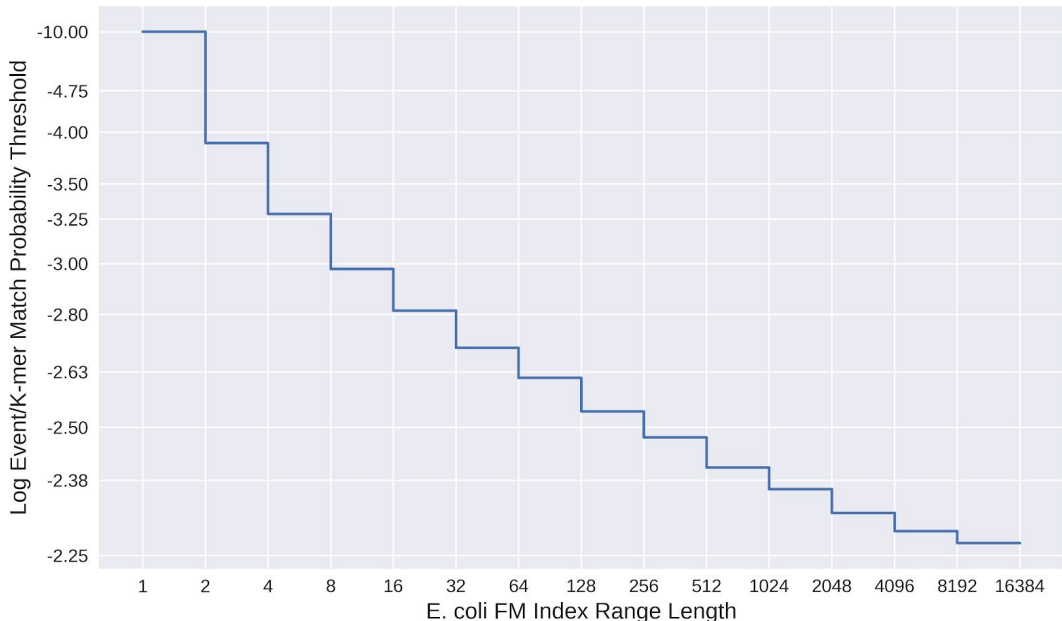


Supplemental Figure S1. FM Index alignment examples. **(top)** FM index alignment of a standard DNA sequence, where the size of each box represents the number of possible locations. **(middle)** FM alignment of a sequence where every position could be one of two bases. Base ambiguity is analogous to the k-mers we consider for every event. **(bottom)** Same as middle but alignments starting from all positions are found by filling in the gaps between ranges from previous alignments.

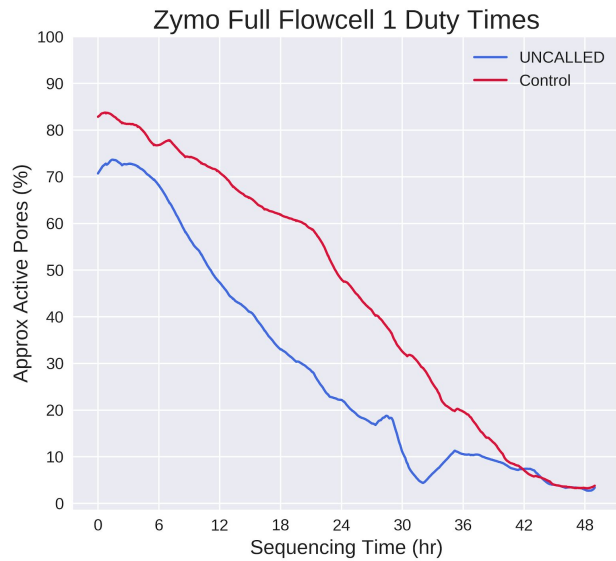
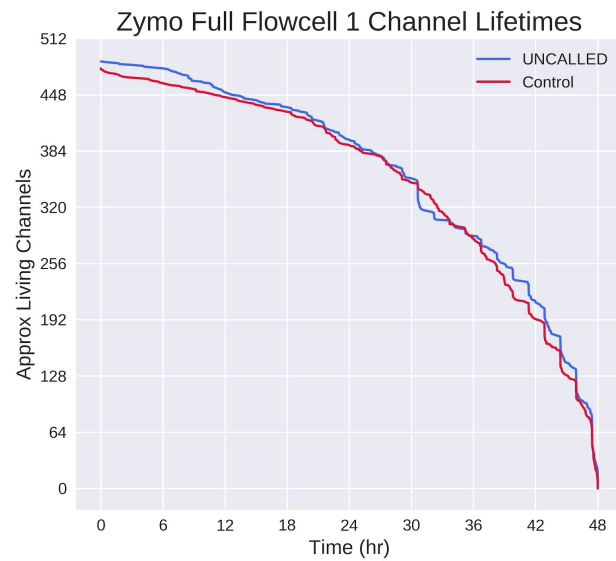
a.



b.

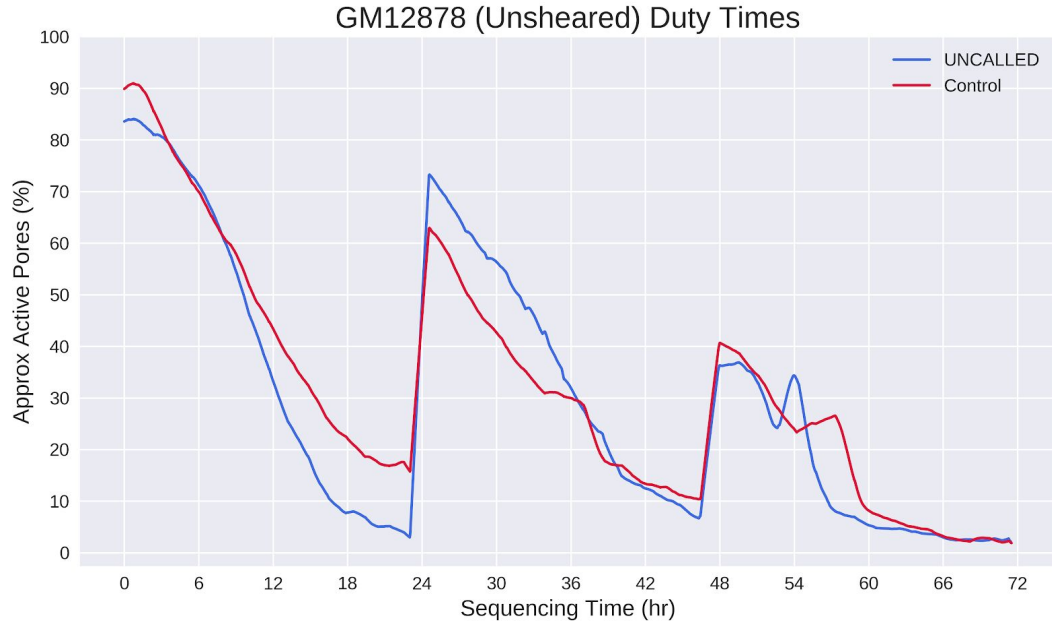


Supplemental Figure S2. Match Probability Thresholds **(a)** Relationship between natural log probability thresholds (x-axis), the mean number of k-mers that match above each threshold per event (blue), the fraction of events that match their correct k-mer above each threshold (red). The values for r9.4 chemistry are shown here. **(b)** The FM index range lengths assigned to different probability thresholds for the *E. coli* reference. This function varies depending on the reference used.

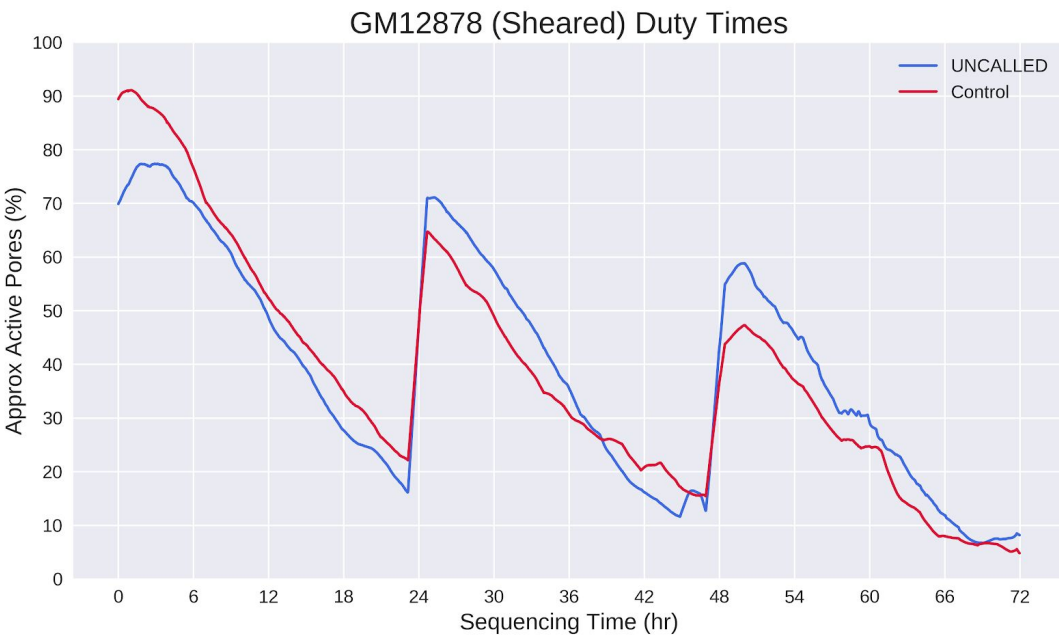
a**b**

Supplemental Figure S3. Pore activity during Zymo “full flowcell 1” sequencing runs. **(a)** Percent of channels that are labeled active throughout zymo bacterial depletion UNCALLED and control runs, based on the percent of signal labeled “pore” or “strand” in the MinKNOW duty times. Curves are smoothed by taking the mean of 92 minute windows, which smooths over mux scans. **(b)** Number of channels which are “alive” throughout the run, meaning they have the capacity to sequence reads, based on when the last read was produced. This is distinct from the duty time plots in that a channel may not produce a read for several hours but still be considered “alive”.

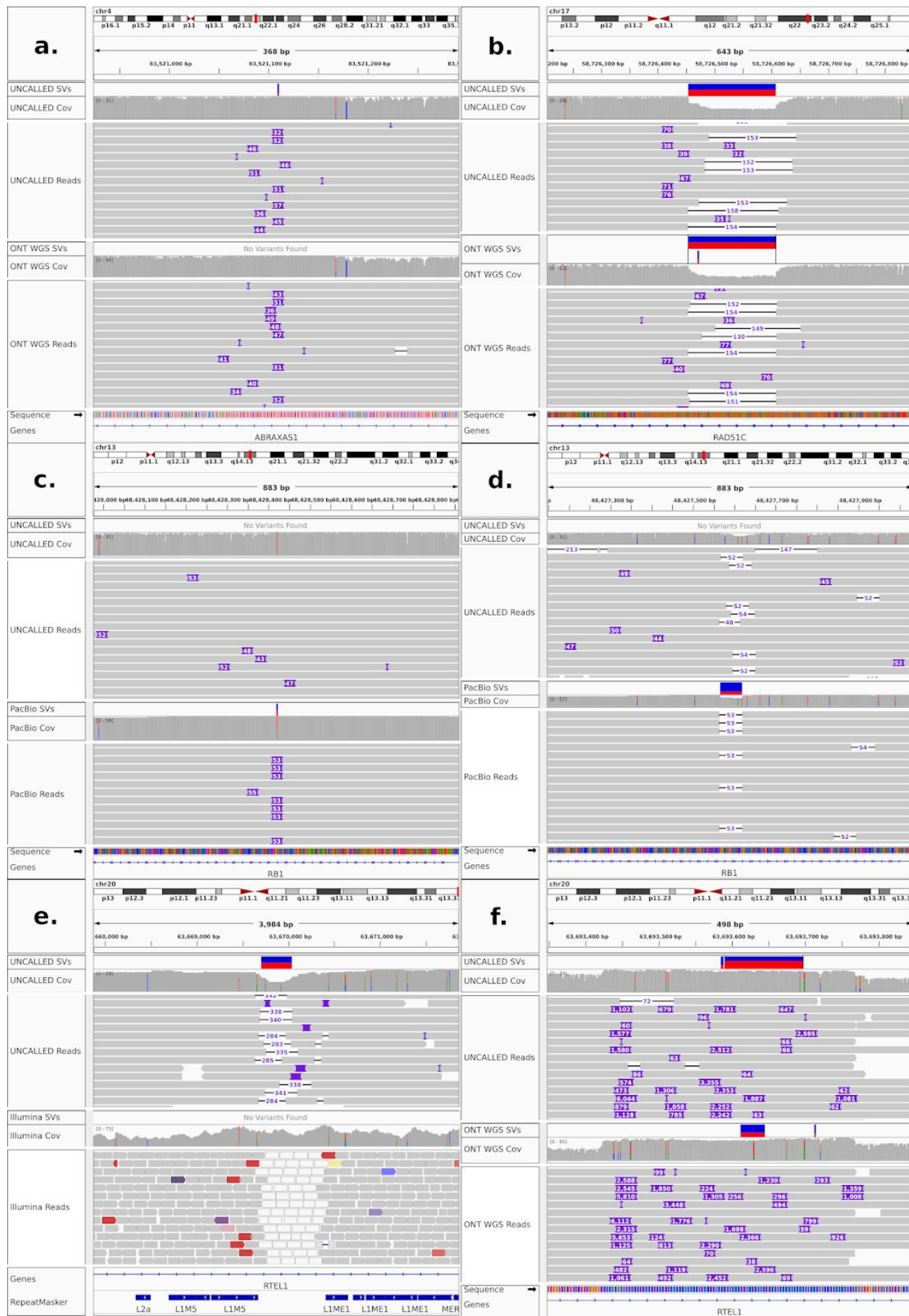
a.



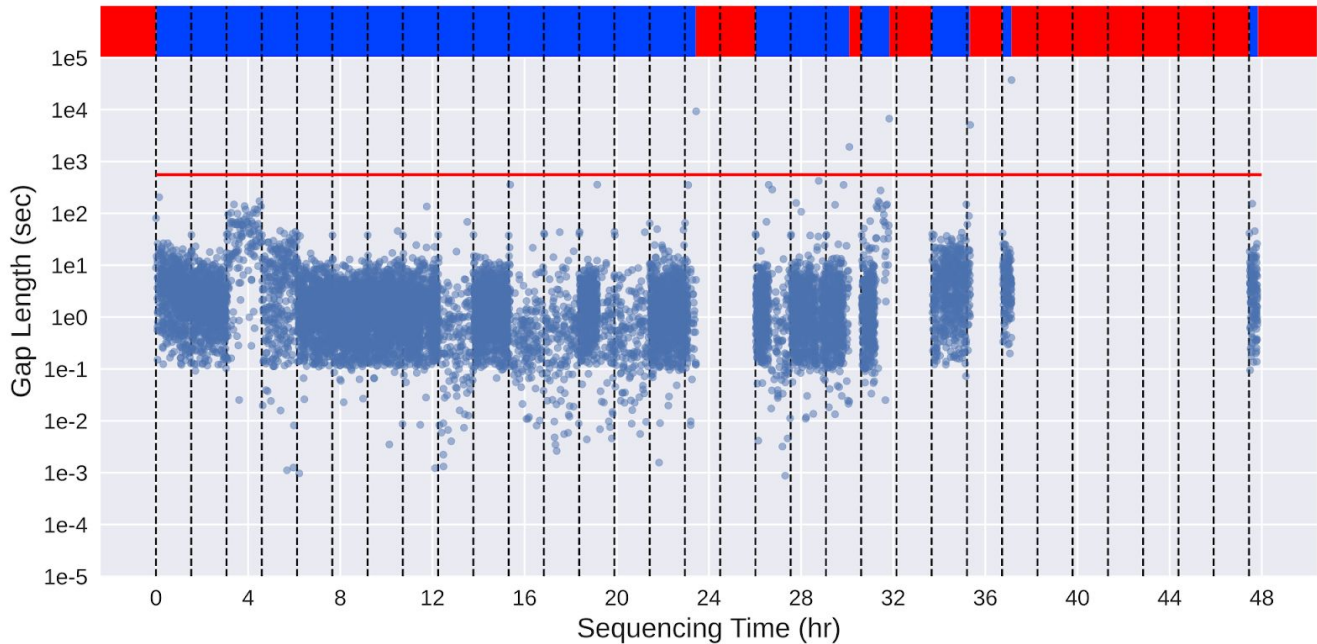
b.



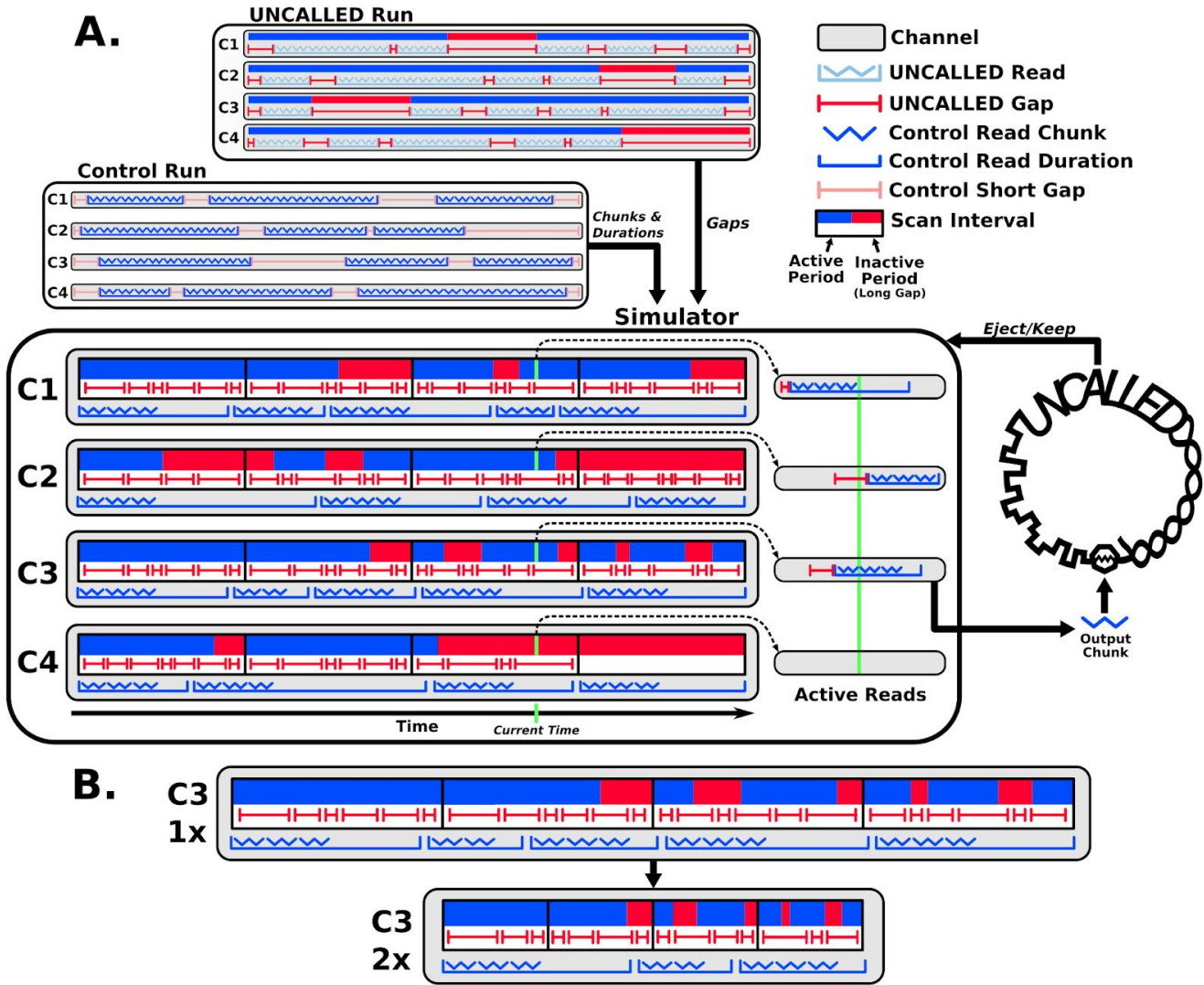
Supplemental Figure S4 GM12878 gene enrichment run duty times in the (a) unsheared run and (b) sheared run. Nuclease flushes were carried out at 24 and 48 hours in both runs. Curves plotted as in **Supplemental Fig. S3**. Note: we observed that a large patch of channels were marked as inactive after the second flush in the sheared UNCALLED run, which can occur because of bubbles introduced when loading.



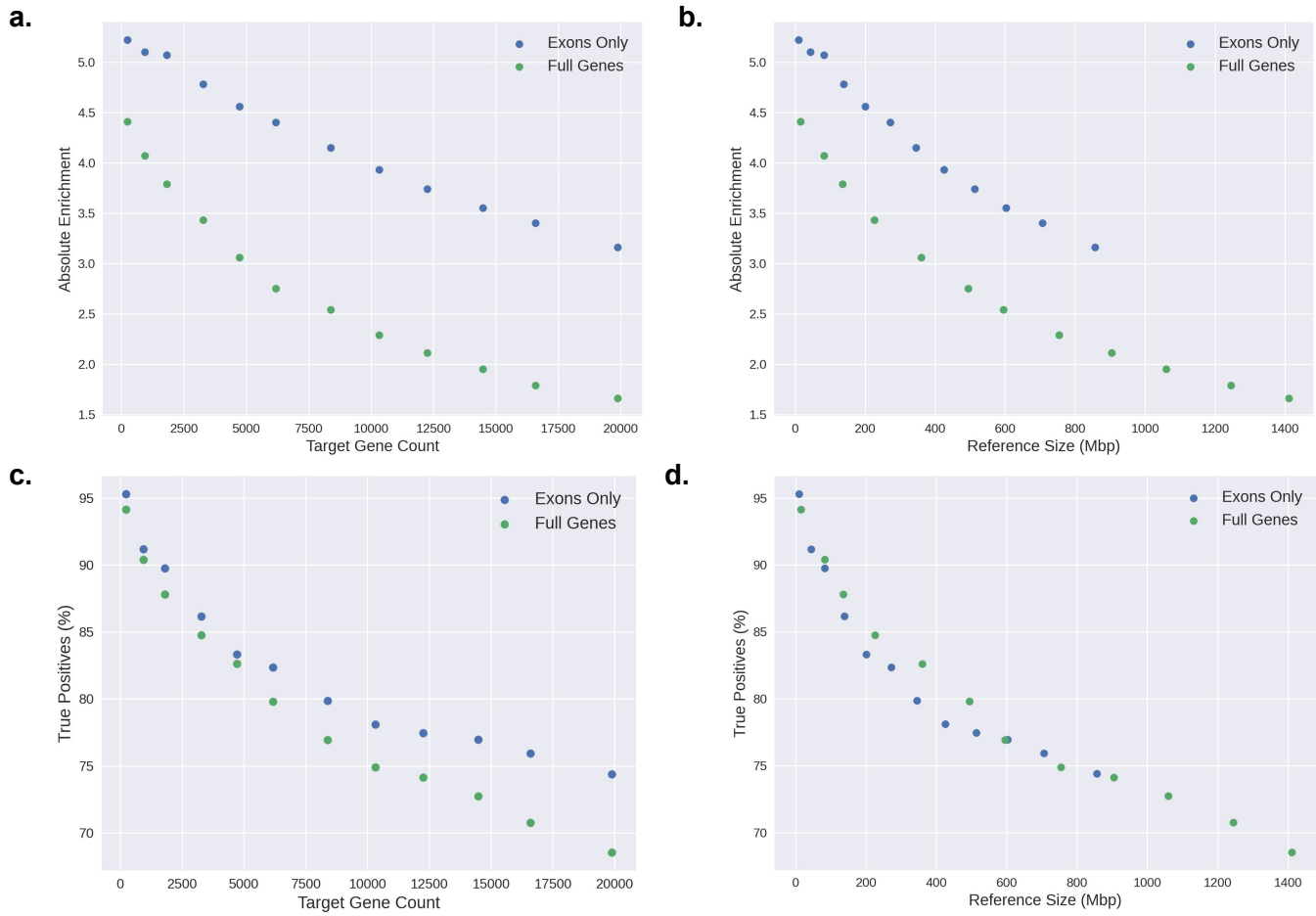
Supplemental Figure S5. SVs confirmed by applying sensitive parameters in Sniffles and SURVIVOR or which required manual inspection to correct. **(a)** Insertion detected by UNCALLED but not by ONT WGS because most reads represented it as < 50bp. **(b)** Insertion detected by ONT WGS but not by UNCALLED because of low-complexity sequence. The overlapping deletion on the other haplotype also likely made the insertion difficult to resolve. **(c)** Insertions detected by UNCALLED but not by PacBio because of low-complexity sequence. **(d)** Deletion detected by PacBio but not by UNCALLED. **(e)** Deletion detected by UNCALLED (and all other long-read datasets) but not by Illumina reads, likely because of surrounding repetitive elements. Note that white read alignments indicate low mapping quality. **(f)** Sniffles called two SVs in this locus in both UNCALLED and ONT WGS, while it appears to represent a single duplication. SURVIVOR merged the ONT WGS SVs but not the UNCALLED SVs, causing a falsely unmatched SV. This is a known issue with SURVIVOR and this case was manually corrected.



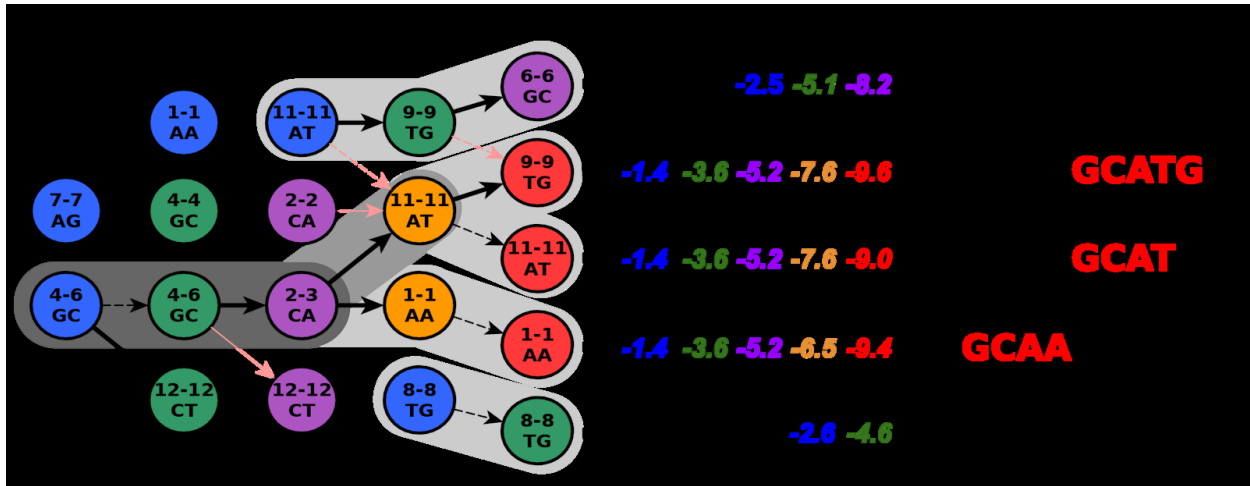
Supplemental Figure S6. Durations of gaps between reads on channel 109 of the Zymo Full Flowcell
 1 UNCALLED run. X-axis indicates when a read ended, Y-axis indicates how long until the next read begins (log scale). Dashed vertical lines indicate mux scans, which often correspond to when gap characteristics change due to pore transitions. The horizontal red line is at one standard deviation over the median gap length for the entire run (including other channels), which is the threshold the simulator uses to define active and inactive periods as represented by the top blue and red bars respectively.



Supplemental Figure S7. (a) Outline of the ReadUntil simulator. Inputs are sequencing summaries of an UNCALLED run and a control run, in addition to the corresponding UNCALLED PAF file and the raw reads from the control run. The overall “pattern” of the simulation is generated from the UNCALLED run: for each channel, gaps between the end of a read and the start of the next are separated into “short” and “long”, where the long gaps are used to define broadly active and inactive periods of the channel (see **Supplementary Fig. S6**) and the short gaps are stored in a series queues, each associated with a scan interval. Scan intervals are periods between two mux scans which are synchronized across all channels. The read chunks and durations are loaded from the control run. **(b)** Illustration of how simulations can be shortened by scaling down the active/inactive periods and scan intervals, but leaving the read and short gap duration unchanged.



Supplemental Figure S8. Simulated results of targeting sets of human genes: (a) absolute enrichment with respect to gene count, (b) absolute enrichment with respect to reference size, (c) true positive rate with respect to gene count, (d) true positive rate with respect to reference size. True positive rates were computed based on reads where the first 1,350bp of each read fully aligns to the target reference according to minimap2. Note that reference size includes the 5Kbp surrounding each gene/exon, while the level of enrichment is calculated based on coverage of the target sequence only (see **Supplemental Table S8**).



Supplemental Figure S9. Representation of alignments in path buffers. The “Virtual Alignment Forest” is a more detailed version of the one in **Fig. 1a**. Pink edges mark paths that were pruned out due to lower probability in order to maintain the tree structure. Shaded backgrounds mark paths that have not been pruned out and are therefore represented in path buffers, and darker shading indicates that part of the path is represented in multiple buffers. “Path Buffers” store cumulative log probabilities that can be used to compute a rolling mean log probability as mapping progresses, as well as “stay” versus “move” events represented by dotted versus solid lines. Seed mappings are inferred from the FM index coordinate which are also stored in the buffers.

References

1. Miga, K. H. *et al.* Telomere-to-telomere assembly of a complete human X chromosome. *bioRxiv* 735928 (2019) doi:10.1101/735928.
2. Sedlazeck, F. J., Lee, H., Darby, C. A. & Schatz, M. C. Piercing the dark matter: bioinformatics of long-range sequencing and mapping. *Nat. Rev. Genet.* **19**, 329–346 (2018).
3. Simpson, J. T. *et al.* Detecting DNA cytosine methylation using nanopore sequencing. *Nat. Methods* **14**, 407–410 (2017).
4. Rang, F. J., Kloosterman, W. P. & de Ridder, J. From squiggle to basepair: computational approaches for improving nanopore sequencing read accuracy. *Genome Biol.* **19**, 90 (2018).
5. Quick, J. *et al.* Real-time, portable genome sequencing for Ebola surveillance. *Nature* **530**, 228–232 (2016).
6. Grädel, C. *et al.* Rapid and Cost-Efficient Enterovirus Genotyping from Clinical Samples Using Flongle Flow Cells. *Genes* **10**, (2019).
7. Sedlazeck, F. J. *et al.* Accurate detection of complex structural variations using single-molecule sequencing. *Nat. Methods* **15**, 461–468 (2018).
8. Luo, R., Sedlazeck, F. J., Lam, T.-W. & Schatz, M. C. A multi-task convolutional deep neural network for variant calling in single molecule sequencing. *Nat. Commun.* **10**, 998 (2019).
9. Rand, A. C. *et al.* Mapping DNA methylation with high-throughput nanopore sequencing. *Nat. Methods* **14**, 411–413 (2017).
10. Gilpatrick, T. *et al.* Targeted Nanopore Sequencing with Cas9 for studies of methylation, structural variants, and mutations. *bioRxiv* 604173 (2019).
11. Loose, M., Malla, S. & Stout, M. Real-time selective sequencing using nanopore technology. *Nat. Methods* **13**, 751–754 (2016).
12. Payne, A., Holmes, N., Rakyan, V. & Loose, M. BulkVis: a graphical viewer for Oxford nanopore bulk FAST5 files. *Bioinformatics* **35**, 2193–2198 (2019).

13. Gu, W. *et al.* Depletion of Abundant Sequences by Hybridization (DASH): using Cas9 to remove unwanted high-abundance species in sequencing libraries and molecular counting applications. *Genome Biol.* **17**, 41 (2016).
14. Edwards, H. S. *et al.* Real-Time Selective Sequencing with RUBRIC: Read Until with Basecall and Reference-Informed Criteria. *Sci. Rep.* **9**, 1–11 (2019).
15. Payne, A. *et al.* Nanopore adaptive sequencing for mixed samples, whole exome capture and targeted panels. *bioRxiv* 2020.02.03.926956 (2020) doi:10.1101/2020.02.03.926956.
16. Ferragina, P. & Manzini, G. Opportunistic data structures with applications. in *Proceedings 41st Annual Symposium on Foundations of Computer Science* 390–398 (2000).
17. Li, H. Minimap2: pairwise alignment for nucleotide sequences. *Bioinformatics* **34**, 3094–3100 (2018).
18. Kurtz, S. *et al.* Versatile and open software for comparing large genomes. *Genome Biol.* **5**, R12 (2004).
19. Shafin, K. *et al.* Efficient de novo assembly of eleven human genomes using PromethION sequencing and a novel nanopore toolkit. *bioRxiv* 715722 (2019) doi:10.1101/715722.
20. Invitae Catalog | Hereditary Cancer. <https://www.invitae.com/en/physician/category/CAT000015/>.
21. NA12878. (Github).
22. Marçais, G. *et al.* MUMmer4: A fast and versatile genome alignment system. *PLoS Comput. Biol.* **14**, e1005944 (2018).
23. Luo, R. *et al.* Clair: Exploring the limit of using a deep neural network on pileup data for germline variant calling. *bioRxiv* 865782 (2019) doi:10.1101/865782.
24. Zook, J. M. *et al.* An open resource for accurately benchmarking small variant and reference calls. *Nat. Biotechnol.* **37**, 561–566 (2019).
25. Cleary, J. G. *et al.* Joint variant and de novo mutation identification on pedigrees from high-throughput sequencing data. *J. Comput. Biol.* **21**, 405–419 (2014).
26. Krusche, P. *et al.* Best practices for benchmarking germline small-variant calls in human genomes.

27. Chen, X. *et al.* Manta: rapid detection of structural variants and indels for germline and cancer sequencing applications. *Bioinformatics* **32**, 1220–1222 (2016).
28. Li, H. & Durbin, R. Fast and accurate long-read alignment with Burrows–Wheeler transform. *Bioinformatics* **26**, 589–595 (2010).
29. Jeffares, D. C. *et al.* Transient structural variations have strong effects on quantitative traits and reproductive isolation in fission yeast. *Nat. Commun.* **8**, 14061 (2017).
30. Tarailo-Graovac, M. & Chen, N. Using RepeatMasker to identify repetitive elements in genomic sequences. *Curr. Protoc. Bioinformatics* **Chapter 4**, Unit 4.10 (2009).
31. Benson, G. Tandem repeats finder: a program to analyze DNA sequences. *Nucleic Acids Res.* **27**, 573–580 (1999).
32. Karolchik, D. *et al.* The UCSC Genome Browser Database. *Nucleic Acids Res.* **31**, 51–54 (2003).
33. Genetics Home Reference. MUTYH gene. *Genetics Home Reference* <https://ghr.nlm.nih.gov/gene/MUTYH>.
34. Deininger, P. Alu elements: know the SINEs. *Genome Biol.* **12**, 236 (2011).
35. Carrel, L. & Willard, H. F. X-inactivation profile reveals extensive variability in X-linked gene expression in females. *Nature* **434**, 400–404 (2005).
36. Forbes, S. A. *et al.* COSMIC: mining complete cancer genomes in the Catalogue of Somatic Mutations in Cancer. *Nucleic Acids Res.* **39**, D945–50 (2011).
37. Gardner, E. J. *et al.* The Mobile Element Locator Tool (MELT): population-scale mobile element discovery and biology. *Genome Res.* **27**, 1916–1929 (2017).
38. Wu, J. *et al.* Tangram: a comprehensive toolbox for mobile element insertion detection. *BMC Genomics* **15**, 795 (2014).
39. Cheadle, J. P. & Sampson, J. R. Exposing the MYtH about base excision repair and human inherited disease. *Hum. Mol. Genet.* **12 Spec No 2**, R159–65 (2003).
40. Win, A. K. *et al.* Risk of colorectal cancer for carriers of mutations in MUTYH, with and without a

family history of cancer. *Gastroenterology* **146**, 1208–11.e1–5 (2014).

41. Nanopore Community Meeting 2019 technology update. *Oxford Nanopore Technologies* <https://nanoporetech.com/resource-centre/nanopore-community-meeting-2019-technology-update> (2019).
42. Roeck, A. D. *et al.* Accurate characterization of expanded tandem repeat length and sequence through whole genome long-read sequencing on PromethION. *bioRxiv* 439026 (2018).
43. David, M., Dursi, L. J., Yao, D., Boutros, P. C. & Simpson, J. T. Nanocall: an open source basecaller for Oxford Nanopore sequencing data. *Bioinformatics* **33**, 49–55 (2017).
44. *kmer_models*. (Github).
45. Welford, B. P. Note on a Method for Calculating Corrected Sums of Squares and Products. *Technometrics* **4**, 419–420 (1962).
46. Langmead, B., Trapnell, C., Pop, M. & Salzberg, S. L. Ultrafast and memory-efficient alignment of short DNA sequences to the human genome. *Genome Biol.* **10**, R25 (2009).
47. Kim, D., Langmead, B. & Salzberg, S. L. HISAT: a fast spliced aligner with low memory requirements. *Nat. Methods* **12**, 357–360 (2015).
48. Gog, S. & Petri, M. Optimized succinct data structures for massive data. *Softw. Pract. Exp.* **44**, 1287–1314 (2014).
49. Li, H. Minimap and miniasm: fast mapping and de novo assembly for noisy long sequences. *Bioinformatics* **32**, 2103–2110 (2016).
50. Yates, A. D. *et al.* Ensembl 2020. *Nucleic Acids Res.* **48**, D682–D688 (2020).
51. Quinlan, A. R. & Hall, I. M. BEDTools: a flexible suite of utilities for comparing genomic features. *Bioinformatics* **26**, 841–842 (2010).
52. Marçais, G. & Kingsford, C. A fast, lock-free approach for efficient parallel counting of occurrences of k-mers. *Bioinformatics* **27**, 764–770 (2011).
53. Aganezov, S. *et al.* Comprehensive analysis of structural variants in breast cancer genomes using

single molecule sequencing. *bioRxiv* 847855 (2019) doi:10.1101/847855.